

The S816, S817, and S818 Airfoils

October 1991 – July 1992

D.M. Somers
Airfoils, Inc.
State College, Pennsylvania



NREL

National Renewable Energy Laboratory
1617 Cole Boulevard, Golden, Colorado 80401-3393
303-275-3000 • www.nrel.gov

Operated for the U.S. Department of Energy
Office of Energy Efficiency and Renewable Energy
by Midwest Research Institute • Battelle

Contract No. DE-AC36-99-GO10337

The S816, S817, and S818 Airfoils

October 1991 – July 1992

D.M. Somers
Airfoils, Inc.
State College, Pennsylvania

NREL Technical Monitor: Jim Tangler

Prepared under Subcontract No. AF-1-11154-1



NREL

National Renewable Energy Laboratory
1617 Cole Boulevard, Golden, Colorado 80401-3393
303-275-3000 • www.nrel.gov

Operated for the U.S. Department of Energy
Office of Energy Efficiency and Renewable Energy
by Midwest Research Institute • Battelle

Contract No. DE-AC36-99-GO10337

**This publication was reproduced from the best available copy
submitted by the subcontractor and received no editorial review at NREL**

NOTICE

This report was prepared as an account of work sponsored by an agency of the United States government. Neither the United States government nor any agency thereof, nor any of their employees, makes any warranty, express or implied, or assumes any legal liability or responsibility for the accuracy, completeness, or usefulness of any information, apparatus, product, or process disclosed, or represents that its use would not infringe privately owned rights. Reference herein to any specific commercial product, process, or service by trade name, trademark, manufacturer, or otherwise does not necessarily constitute or imply its endorsement, recommendation, or favoring by the United States government or any agency thereof. The views and opinions of authors expressed herein do not necessarily state or reflect those of the United States government or any agency thereof.

Available electronically at <http://www.osti.gov/bridge>

Available for a processing fee to U.S. Department of Energy
and its contractors, in paper, from:

U.S. Department of Energy
Office of Scientific and Technical Information
P.O. Box 62
Oak Ridge, TN 37831-0062
phone: 865.576.8401
fax: 865.576.5728
email: <mailto:reports@adonis.osti.gov>

Available for sale to the public, in paper, from:

U.S. Department of Commerce
National Technical Information Service
5285 Port Royal Road
Springfield, VA 22161
phone: 800.553.6847
fax: 703.605.6900
email: orders@ntis.fedworld.gov
online ordering: <http://www.ntis.gov/ordering.htm>



Table of Contents

Abstract.....	1
Introduction.....	1
Symbols.....	1
Airfoil Design.....	2
Objectives and Constraints	2
Philosophy.....	3
Execution	6
Discussion of Results.....	6
S816	6
S817	8
S818	9
Concluding Remarks.....	10
References.....	10

List of Tables

Table I. Airfoil Design Specifications	12
Table II. S816 Airfoil Coordinates	13
Table III. S817 Airfoil Coordinates.....	14
Table IV. S818 Airfoil Coordinates.....	15

List of Figures

Figure 1: Airfoil shapes	16
Figure 2: Inviscid pressure distributions for S816 airfoil	17 – 21
Figure 3: Section characteristics of S816 airfoil.....	22 – 26
Figure 4: Inviscid pressure distributions for S817 airfoil	27 – 31
Figure 5: Section Characteristics of S817 airfoil.....	33 – 36
Figure 6: Inviscid Pressure distribution for S818 airfoil	37 – 43
Figure 7: Section characteristics of S818 airfoil	44 – 48

THE S816, S817, AND S818 AIRFOILS

Dan M. Somers

July 1992

ABSTRACT

A family of thick laminar-flow airfoils for 30- to 40-meter horizontal-axis wind turbines, the S816, S817, and S818, has been designed and analyzed theoretically. The primary objectives of restrained maximum lift, insensitive to roughness, and low profile drag have been achieved. The constraints on the pitching moments and airfoil thicknesses have been satisfied.

INTRODUCTION

The family of thick laminar-flow airfoils designed under this study is intended for 30- to 40-meter horizontal-axis wind turbines. An earlier thick-airfoil family, the S809, S810, and S811 (ref. 1), was designed for 20-meter rotors.

The specific tasks performed under this study are described in Solar Energy Research Institute (SERI) Subcontract Number AF-1-11154-1. The initial specifications for the airfoils are outlined in the Statement of Work, dated 30 August 1991. These specifications were later refined during telephone conversations with Mr. James L. Tangler of the National Renewable Energy Laboratory (NREL), formerly SERI.

Because of the limitations of the theoretical methods (refs. 2 and 3) employed in this study, the results presented are in no way guaranteed to be accurate—either in an absolute or in a relative sense. This statement applies to the entire study.

SYMBOLS

C_p	pressure coefficient
c	airfoil chord
c_d	section profile-drag coefficient
c_l	section lift coefficient

c_m	section pitching-moment coefficient about quarter-chord point
L.	lower surface
MU	transition mode (ref. 3)
R	Reynolds number based on free-stream conditions and airfoil chord
S.	separation location, $1 - s_{sep}/c$
s_{sep}	arc length along which boundary layer is separated
s_{turb}	arc length along which boundary layer is turbulent including s_{sep}
T.	transition location, $1 - s_{turb}/c$
U.	upper surface
x	airfoil abscissa
y	airfoil ordinate
α	angle of attack relative to chord line, degrees

AIRFOIL DESIGN

OBJECTIVES AND CONSTRAINTS

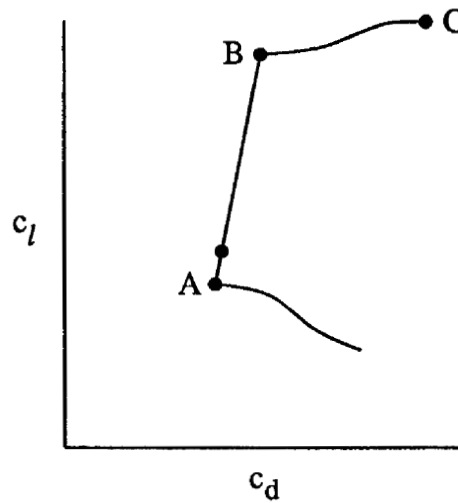
The design specifications for the family of airfoils are contained in table I. The family consists of three airfoils—primary, tip, and root—corresponding to the 0.75, 0.95, and 0.40 blade radial stations, respectively.

Two primary objectives are evident from the specifications. The first objective is to obtain maximum lift coefficients, for the primary and tip airfoils, which are relatively low (restrained). In contrast, the maximum lift coefficient for the root airfoil should be as high as possible. A requirement related to this objective is that the maximum lift coefficient not decrease with transition fixed near the leading edge on both surfaces. The second objective is to obtain low profile-drag coefficients over the ranges of lift coefficients from 0.4 to 1.0 for the primary airfoil, from 0.3 to 0.9 for the tip airfoil, and from 0.6 to 1.2 for the root airfoil.

Two major constraints were placed on the design of these airfoils. First, the zero-lift pitching-moment coefficients must be no more negative than -0.07 for the primary and tip airfoils and -0.15 for the root airfoil. Second, the airfoil thicknesses must equal 21-percent chord for the primary airfoil, 16-percent chord for the tip airfoil, and 24-percent chord for the root airfoil.

PHILOSOPHY

Given the above objectives and constraints, certain characteristics of the designs are evident. The following sketch illustrates a drag polar which meets the goals for these designs.

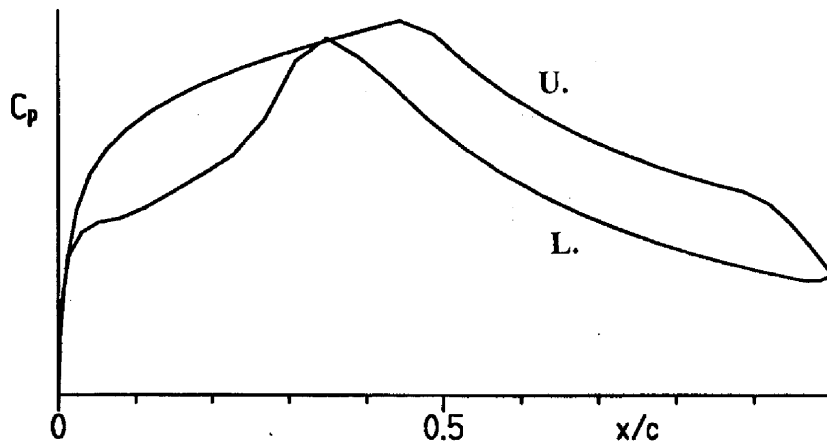


Sketch 1

The desired airfoil shapes can be traced to the pressure distributions which occur at the various points in the sketch. Point A is the lower limit of the low-drag lift-coefficient range. The lift coefficient at point A is 0.1 lower than the objective specified in table I. The difference is intended as a margin against such contingencies as manufacturing tolerances, operational deviations, three-dimensional effects, and inaccuracies in the theoretical method. The drag at point B, the upper limit of the low-drag lift-coefficient range, is not as low as at point A, unlike the polars of many other laminar-flow airfoils where the drag within the laminar bucket is nearly constant. This characteristic is related to the elimination of significant (drag-producing) laminar separation bubbles on the upper surface. (See ref. 4.) It is acceptable because the ratio of the profile drag to the total drag of the wind-turbine blade decreases with increasing lift coefficient. A 0.1-lift-coefficient margin against contingencies is not possible at the upper limit of the low-drag lift-coefficient range because of the proximity of the upper limit to the maximum lift coefficient. As large a margin as possible is sought, however. The drag increases very rapidly outside the laminar bucket because the transition point moves quickly toward the leading edge. This feature results in a rather sharp leading edge which produces a suction peak at higher lift coefficients, which limits

the maximum lift coefficient and ensures that transition will occur very near the leading edge. Thus, the maximum lift coefficient occurs with turbulent flow along the entire upper surface and, therefore, should be insensitive to roughness at the leading edge. Point C is the maximum lift coefficient.

From the preceding discussion, the pressure distributions along the polar can be deduced. The pressure distribution at point A for the primary airfoil should look something like the following. (The pressure distributions for the tip and root airfoils should be qualitatively similar.)



Sketch 2

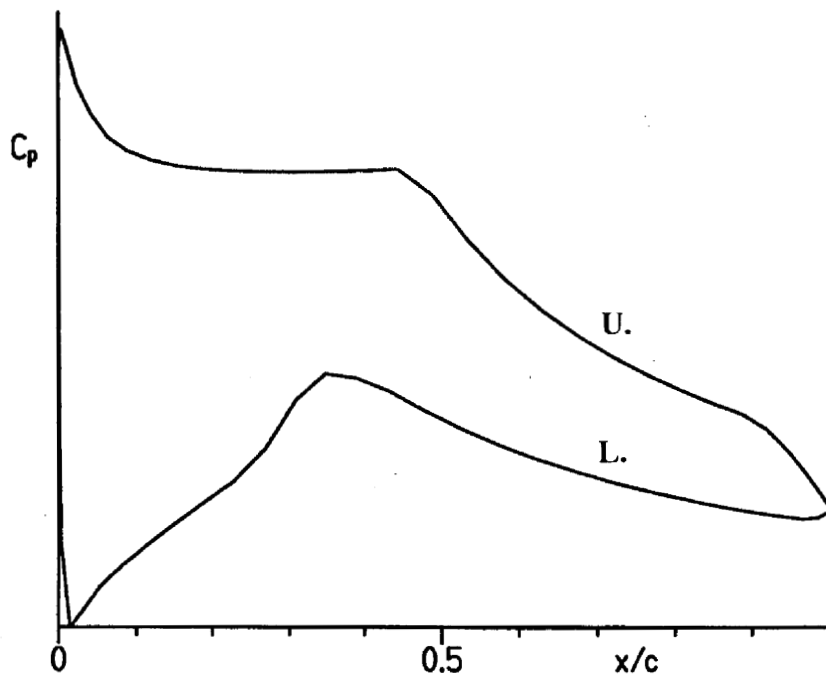
To achieve low drag, a favorable pressure gradient is desirable along the upper surface to about 45-percent chord. Aft of this point, a short region of adverse pressure gradient (“transition ramp”) is desirable to promote the efficient transition from laminar to turbulent flow (ref. 5). Thus, the initial slope of the pressure recovery is relatively shallow. This short region is followed by a steeper concave pressure recovery. The specific concave pressure recovery employed represents a compromise among maximum lift, low drag, and docile stall characteristics. The steep adverse pressure gradient on the upper surface aft of about 90-percent chord is a ‘separation ramp,’ originally proposed by F. X. Wortmann, which confines turbulent separation to a small region near the trailing edge. By controlling the movement of the separation point at high angles of attack, high lift coefficients can be achieved with little drag penalty. This feature has the added benefit that it too promotes docile stall characteristics. (See ref. 6.)

A favorable pressure gradient is desirable along the lower surface to about 35-percent chord to achieve low drag. The pressure gradients along the forward portion of the lower surface increase the amount of camber in the leading-edge region while maintaining low drag at the lower limit of the laminar bucket. The forward camber serves to balance, with respect to the pitching-

moment constraint, the aft camber, both of which contribute to the achievement of the maximum lift coefficient. This region is followed by a curved transition ramp (ref. 4) which is longer than that on the upper surface. The transition ramp is followed by a concave pressure recovery which produces lower drag and has less tendency to separate than the corresponding linear or convex pressure recovery. The pressure recovery must begin relatively far forward to alleviate lower-surface separation at lower lift coefficients.

The amounts of pressure recovery on the two surfaces are determined by the airfoil-thickness and pitching-moment constraints.

At point B, the pressure distribution should look like this:



Sketch 3

No suction spike exists at the leading edge. Instead, the peak occurs just aft of the leading edge. This feature results from incorporating increasingly favorable pressure gradients toward the leading edge. It allows a wider laminar bucket to be achieved and higher lift coefficients to be reached without significant separation.

EXECUTION

Given the pressure distributions previously discussed, the design of the airfoils is reduced to the inverse problem of transforming the pressure distributions into airfoil shapes. The Eppler Code (refs. 2 and 3) was used because of confidence gained during the design, analysis, and experimental verification of several other airfoils. (See refs. 7-9.)

The primary airfoil is designated the S816. The tip airfoil, the S817, and the root airfoil, the S818, were derived from the S816 to increase the aerodynamic and geometric compatibilities of the three airfoils. The airfoil shapes are shown in figure 1 and the coordinates are contained in tables II, III, and IV. The S816 airfoil thickness is 21-percent chord; the S817, 16-percent chord; and the S818, 24-percent chord.

DISCUSSION OF RESULTS

S816

Pressure Distributions

The inviscid (potential-flow) pressure distributions for the S816 airfoil for various angles of attack are shown in figure 2. Because the free-stream Mach number for all relevant operating conditions remains below 0.2, these and all subsequent results are incompressible.

Transition and Separation Locations

The variation of transition location with lift coefficient for the S816 airfoil is shown in figure 3. It should be remembered that the method of references 2 and 3 'defines' the transition location as the end of the laminar boundary layer whether due to natural transition or laminar separation. Thus, for conditions which result in relatively long laminar separation bubbles (low lift coefficients for the upper surface and high lift coefficients for the lower surface and/or low Reynolds numbers), poor agreement between the predicted 'transition' locations and the locations measured experimentally can be expected. This poor agreement is worsened by the fact that transition is normally confirmed in the wind tunnel only by the detection of attached turbulent flow. For conditions which result in shorter laminar separation bubbles (high lift coefficients for the upper surface and low lift coefficients for the lower surface and/or high Reynolds numbers), the agreement between theory and experiment should be quite good. (See ref. 10.)

The variation of turbulent-separation location with lift coefficient for the S816 airfoil is shown in figure 3. A small separation is predicted on the upper surface at higher lift coefficients. This separation, which is caused by the separation ramp (fig. 2), increases in length with transition

fixed near the leading edge. Separation is predicted on the lower surface at lift coefficients below about 0 with transition free and at lift coefficients below about 0.4 with transition fixed. The lower-surface separation is not considered important because it occurs at lift coefficients which are not typical of normal wind-turbine operations. Also, such separation usually has little effect on the section characteristics. (See ref. 10.)

Section Characteristics

Reynolds number effects.- The section characteristics of the S816 airfoil are shown in figure 3. It should be noted that the maximum lift coefficient predicted by the method of references 2 and 3 is not always realistic. Accordingly, an empirical criterion should be applied to the computed results. This criterion assumes that the maximum lift coefficient has been reached if the drag coefficient of the upper surface is greater than 0.0240 or if the length of turbulent separation along the upper surface is greater than 0.10. Thus, the maximum lift coefficient for the design Reynolds number of 4.0×10^6 is predicted to be 1.20, which meets the design objective. Based on the movement of the upper-surface separation point, the stall characteristics are expected to be docile. Low drag coefficients are predicted over the range of lift coefficients from 0 to about 1.0, which exceeds the range specified (0.4 to 1.0). The drag coefficient at the specified lower limit of the laminar bucket ($c_l = 0.4$) is predicted to be 0.0062, which is 23 percent below the design objective. The zero-lift pitching-moment coefficient is predicted to be -0.0778 which exceeds the design constraint. However, the method of references 2 and 3 generally overpredicts the pitching-moment coefficient by about 10 percent. Thus, the actual zero-lift pitching-moment coefficient should be about -0.07 , which satisfies the constraint.

An additional analysis (not shown) indicates that significant (drag-producing) laminar separation bubbles should not occur on either surface for any relevant operating condition.

Effect of roughness.- The effect of roughness on the section characteristics of the S816 airfoil is shown in figure 3. Transition was fixed at 2-percent chord on the upper surface and 5-percent chord on the lower surface using transition mode $MU = 1$ (ref. 3). The maximum lift coefficient is unaffected by fixing transition at these locations because transition is predicted to occur forward of 2-percent chord on the upper surface at the maximum lift coefficient. The 'rough' results were obtained using transition mode $MU = 9$ (ref. 3), which simulates distributed roughness due to, for example, leading-edge contamination by insects or rain. At the higher lift coefficients, this transition mode is probably comparable to NACA (National Advisory Committee for Aeronautics) Standard Roughness which "is considerably more severe than that caused by the usual manufacturing irregularities or deterioration in service" (ref. 11). For the rough condition, the maximum lift coefficient for the design Reynolds number of 4.0×10^6 is predicted to be 1.17, a reduction of three percent from that for the transition-free condition. Thus, one of the most important design requirements has been achieved. The drag coefficients are, of course, adversely affected by the roughness.

S817

Pressure Distributions

The inviscid (potential-flow) pressure distributions for the S817 airfoil for various angles of attack are shown in figure 4.

Transition and Separation Locations

The variations of transition and turbulent-separation locations with lift coefficient for the S817 airfoil are shown in figure 5. A small separation is predicted on the upper surface at higher lift coefficients. This separation, which is caused by the separation ramp (fig. 4), increases in length with transition fixed near the leading edge.

Section Characteristics

Reynolds number effects.- The section characteristics of the S817 airfoil are shown in figure 5. Using the previously-described empirical criterion, the maximum lift coefficient for the design Reynolds number of 3.0×10^6 is predicted to be 1.10, which meets the design objective. The stall characteristics are expected to be docile. Low drag coefficients are predicted over the range of lift coefficients from about 0.2 to about 1.0, which exceeds the range specified (0.3 to 0.9). The drag coefficient at the specified lower limit of the laminar bucket ($c_l = 0.3$) is predicted to be 0.0047, which is 33 percent below the design objective. The zero-lift pitching-moment coefficient is predicted to be -0.0778 , which exceeds the design constraint. Again, because the method of references 2 and 3 overpredicts the pitching-moment coefficient, the actual zero-lift pitching-moment coefficient should be about -0.07 , which satisfies the constraint.

An additional analysis (not shown) indicates that significant (drag-producing) laminar separation bubbles should not occur on either surface for any relevant operating condition.

Effect of roughness.- The effect of roughness on the section characteristics of the S817 airfoil is shown in figure 5. Transition was fixed at 2-percent chord on the upper surface and 5-percent chord on the lower surface using transition mode $MU = 1$ (ref. 3). The maximum lift coefficient is unaffected by fixing transition at these locations because transition is predicted to occur forward of 2-percent chord on the upper surface at the maximum lift coefficient. For the rough condition ($MU = 9$), the maximum lift coefficient for the design Reynolds number of 3.0×10^6 is predicted to be 1.08, a reduction of two percent from that for the transition-free condition. Thus, one of the most important design requirements has been achieved. The drag coefficients are, of course, adversely affected by the roughness.

S818

Pressure Distributions

The inviscid (potential-flow) pressure distributions for the S818 airfoil for various angles of attack are shown in figure 6.

Transition and Separation Locations

The variations of transition and turbulent-separation locations with lift coefficient for the S818 airfoil are shown in figure 7. A small separation is predicted on the upper surface at all lift coefficients. This separation, which is caused by the separation ramp (fig. 6), increases in length with transition fixed near the leading edge. Separation is predicted on the lower surface at lower lift coefficients. Such separation usually has little effect on the section characteristics.

Section Characteristics

Reynolds number effects.- The section characteristics of the S818 airfoil are shown in figure 7. Using the previously-described empirical criterion, the maximum lift coefficient for the design Reynolds number of 2.5×10^6 is predicted to be 1.68, which exceeds the design objective by 29 percent. The stall characteristics are expected to be docile. Low drag coefficients are predicted over the range of lift coefficients from 0 to about 1.5, which exceeds the range specified (0.6 to 1.2). The drag coefficient at the specified lower limit of the laminar bucket ($c_l = 0.6$) is predicted to be 0.0092, which is 23 percent below the design objective. The zero-lift pitching-moment coefficient is predicted to be -0.1666 , which exceeds the design constraint. Again, because the method of references 2 and 3 overpredicts the pitching-moment coefficient, the actual zero-lift pitching-moment coefficient should be about -0.15 , which satisfies the constraint.

An additional analysis (not shown) indicates that significant (drag-producing) laminar separation bubbles should not occur on either surface for any relevant operating condition.

Effect of roughness.- The effect of roughness on the section characteristics of the S818 airfoil is shown in figure 7. Transition was fixed at 2-percent chord on the upper surface and 5-percent chord on the lower surface using transition mode $MU = 1$ (ref. 3). The maximum lift coefficient is unaffected by fixing transition at these locations because transition is predicted to occur forward of 2-percent chord on the upper surface at the maximum lift coefficient. For the rough condition ($MU = 9$), the maximum lift coefficient for the design Reynolds number of 2.5×10^6 is predicted to be 1.61, a reduction of four percent from that for the transition-free condition. Thus, one of the most important design requirements has been achieved. The drag coefficients are, of course, adversely affected by the roughness.

CONCLUDING REMARKS

A family of thick laminar-flow airfoils for 30- to 40-meter horizontal-axis wind turbines, the S816, S817, and S818, has been designed and analyzed theoretically. The primary objectives of restrained maximum lift coefficients, insensitive to roughness, and low profile-drag coefficients have been achieved. The constraints on the pitching-moment coefficients and airfoil thicknesses have been satisfied.

REFERENCES

1. Somers, Dan M.: The S809 through S813 Airfoils. Airfoils, Inc., 1988.
2. Eppler, Richard: Airfoil Design and Data. Springer-Verlag (Berlin), 1990.
3. Eppler, R.: Airfoil Program System. User's Guide. R. Eppler, c.1991.
4. Eppler, Richard; and Somers, Dan M.: Airfoil Design for Reynolds Numbers Between 50,000 and 500,000. Proceedings of the Conference on Low Reynolds Number Airfoil Aerodynamics, UNDAS-CP-77B123, Univ. of Notre Dame, June 1985, pp. 1-14.
5. Wortmann, F. X.: Experimental Investigations on New Laminar Profiles for Gliders and Helicopters. TIL/T.4906, British Minist. Aviat., Mar. 1960. (Translated from Z. Flugwissenschaften, Bd. 5, Heft 8, Aug. 1957, pp. 228-243.)
6. Maughmer, Mark D.; and Somers, Dan M.: Design and Experimental Results for a High-Altitude, Long-Endurance Airfoil. J. Aircr., vol. 26, no. 2, Feb. 1989, pp. 148-153.
7. Somers, Dan M.: Design and Experimental Results for the S809 Airfoil. Airfoils, Inc., 1989.
8. Somers, Dan M.: Design and Experimental Results for the S805 Airfoil. Airfoils, Inc., 1988.
9. Somers, Dan M.: Subsonic Natural-Laminar-Flow Airfoils. Natural Laminar Flow and Laminar Flow Control, R. W. Barnwell and M. Y. Hussaini, eds., Springer-Verlag New York, Inc., 1992, pp. 143-176.
10. Somers, Dan M.: Design and Experimental Results for a Natural-Laminar-Flow Airfoil for General Aviation Applications. NASA TP-1861, 1981.

11. Abbott, Ira H.; Von Doenhoff, Albert E.; and Stivers, Louis S., Jr.: Summary of Airfoil Data. NACA Rep. 824, 1945. (Supersedes NACA WR L-560.)

TABLE I.- AIRFOIL DESIGN SPECIFICATIONS

<u>Parameter</u>	<u>Objective/Constraint</u>		
	Primary	Tip	Root
Airfoil			
Blade radial station	0.75	0.95	0.40
Reynolds number	4.0×10^6	3.0×10^6	2.5×10^6
Maximum lift coefficient	1.20	1.10	≥ 1.30
Low-drag lift-coefficient range:			
Lower limit	0.4	0.3	0.6
Upper limit	1.0	0.9	1.2
Minimum profile-drag coefficient	0.0080	0.0070	0.0120
Zero-lift pitching-moment coefficient	≥ -0.07	≥ -0.07	≥ -0.15
Thickness	0.21c	0.16c	0.24c

TABLE II.- S816 AIRFOIL COORDINATES

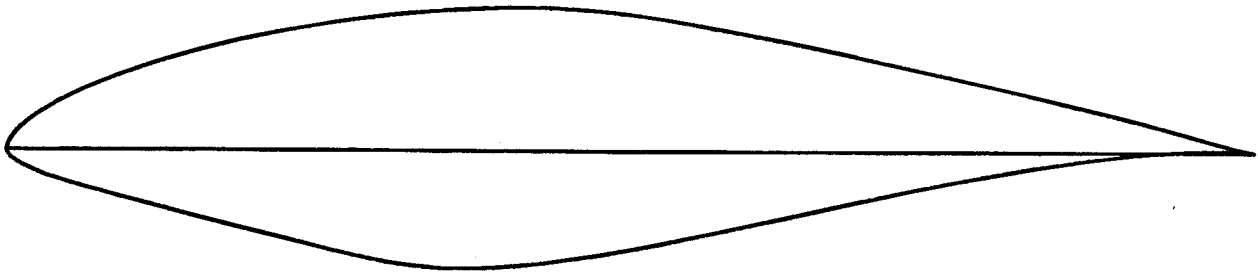
Upper Surface		Lower Surface	
x/c	y/c	x/c	y/c
0.00000	0.00009	0.00019	-0.00158
.00023	.00198	.00093	-.00314
.00302	.00863	.00220	-.00475
.01099	.01818	.00368	-.00620
.02379	.02836	.01412	-.01294
.04125	.03888	.03050	-.01988
.06315	.04950	.05260	-.02698
.08920	.06005	.08019	-.03456
.11901	.07033	.11247	-.04309
.15222	.08009	.14831	-.05249
.18843	.08912	.18682	-.06232
.22723	.09720	.22730	-.07231
.26818	.10411	.26846	-.08222
.31082	.10965	.30881	-.09050
.35467	.11360	.34877	-.09483
.39923	.11569	.39005	-.09470
.44398	.11547	.43340	-.09089
.48900	.11217	.47890	-.08411
.53503	.10591	.52644	-.07515
.58217	.09767	.57555	-.06477
.62982	.08824	.62567	-.05360
.67730	.07811	.67615	-.04229
.72392	.06774	.72622	-.03146
.76893	.05749	.77501	-.02165
.81158	.04763	.82154	-.01331
.85113	.03838	.86477	-.00676
.88685	.02976	.90364	-.00216
.91827	.02165	.93713	.00052
.94534	.01412	.96426	.00150
.96784	.00776	.98412	.00118
.98512	.00320	.99605	.00038
.99617	.00072	1.00000	.00000
1.00000	.00000		

TABLE III.- S817 AIRFOIL COORDINATES

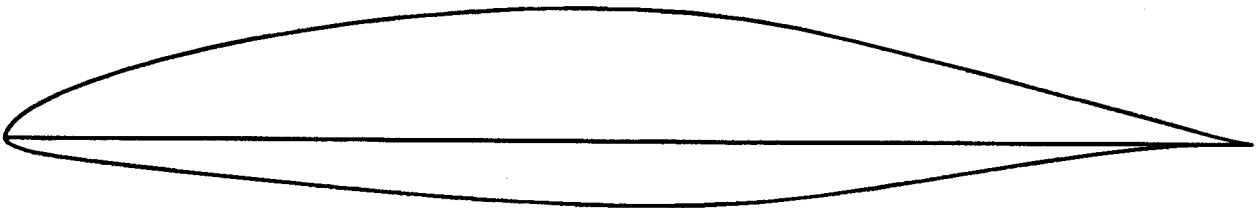
Upper Surface		Lower Surface	
x/c	y/c	x/c	y/c
0.00010	0.00117	0.00001	-0.00038
.00036	.00243	.00029	-.00169
.00443	.01001	.00107	-.00285
.01313	.01841	.00235	-.00398
.02661	.02718	.00925	-.00755
.04479	.03620	.02330	-.01157
.06748	.04533	.04329	-.01517
.09441	.05445	.06911	-.01857
.12517	.06342	.10030	-.02217
.15941	.07203	.13611	-.02613
.19672	.08010	.17584	-.03033
.23667	.08746	.21884	-.03464
.27883	.09392	.26447	-.03891
.32273	.09934	.31211	-.04294
.36790	.10355	.36113	-.04655
.41384	.10640	.41092	-.04952
.46005	.10771	.46088	-.05162
.50602	.10727	.51041	-.05260
.55134	.10473	.55893	-.05200
.59585	.09969	.60634	-.04913
.63984	.09191	.65317	-.04392
.68387	.08192	.69967	-.03701
.72779	.07087	.74564	-.02924
.77085	.05960	.79051	-.02150
.81221	.04865	.83342	-.01447
.85106	.03842	.87341	-.00861
.88653	.02908	.90948	-.00420
.91803	.02060	.94065	-.00132
.94528	.01309	.96599	.00013
.96792	.00701	.98470	.00046
.98522	.00281	.99615	.00020
.99621	.00061	1.00000	.00000
1.00000	.00000		

TABLE IV.- S818 AIRFOIL COORDINATES

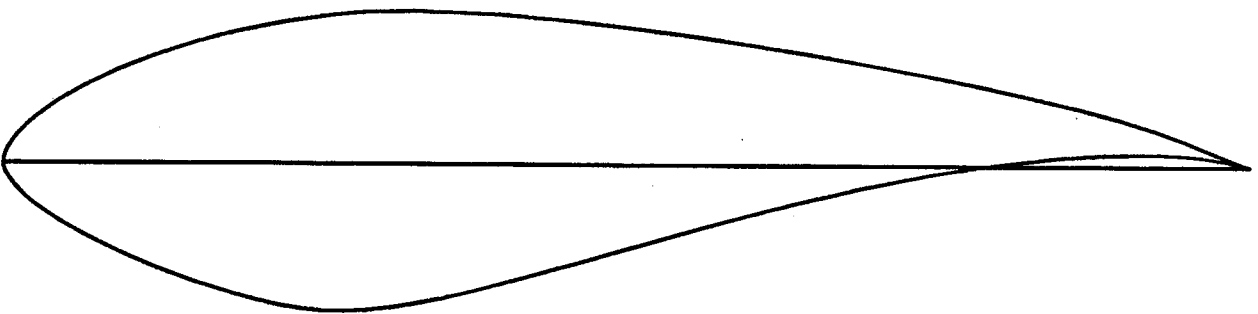
Upper Surface		Lower Surface	
x/c	y/c	x/c	y/c
0.00012	0.00170	0.00003	-0.00087
.00066	.00442	.00048	-.00341
.00374	.01205	.00141	-.00608
.01259	.02437	.00328	-.00985
.02619	.03717	.01232	-.02157
.04424	.05009	.02631	-.03391
.06647	.06284	.04486	-.04650
.09256	.07518	.06764	-.05923
.12213	.08681	.09404	-.07200
.15482	.09745	.12331	-.08444
.19023	.10678	.15489	-.09598
.22797	.11449	.18823	-.10622
.26760	.12006	.22238	-.11444
.30915	.12285	.25700	-.11893
.35312	.12287	.29323	-.11847
.39944	.12073	.33232	-.11328
.44760	.11690	.37488	-.10412
.49702	.11165	.42102	-.09200
.54711	.10527	.47043	-.07786
.59727	.09798	.52267	-.06258
.64685	.09003	.57709	-.04706
.69521	.08161	.63288	-.03217
.74169	.07292	.68903	-.01872
.78569	.06409	.74437	-.00740
.82657	.05526	.79758	.00128
.86377	.04651	.84726	.00704
.89672	.03779	.89200	.00985
.92522	.02885	.93046	.00996
.94958	.01983	.96144	.00780
.96996	.01155	.98351	.00422
.98590	.00509	.99606	.00113
.99633	.00122	1.00000	.00000
1.00000	.00000		



(a) S816.

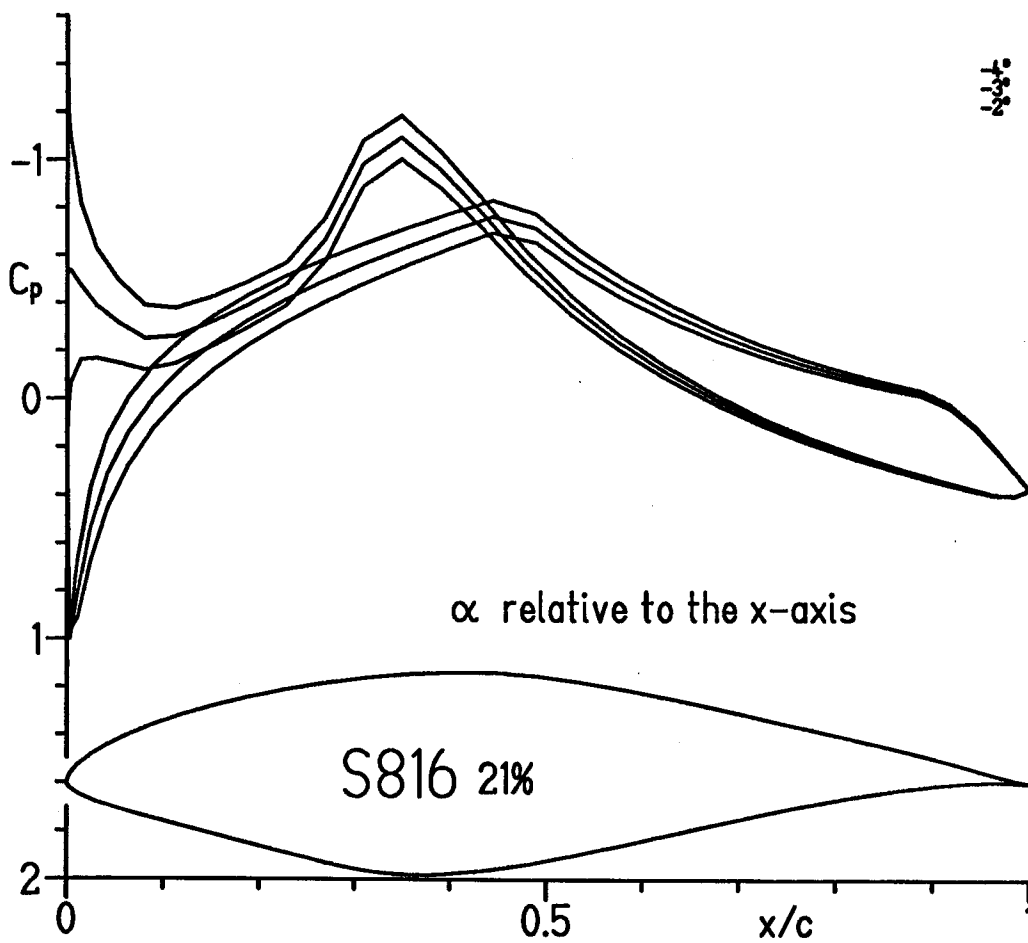


(b) S817.



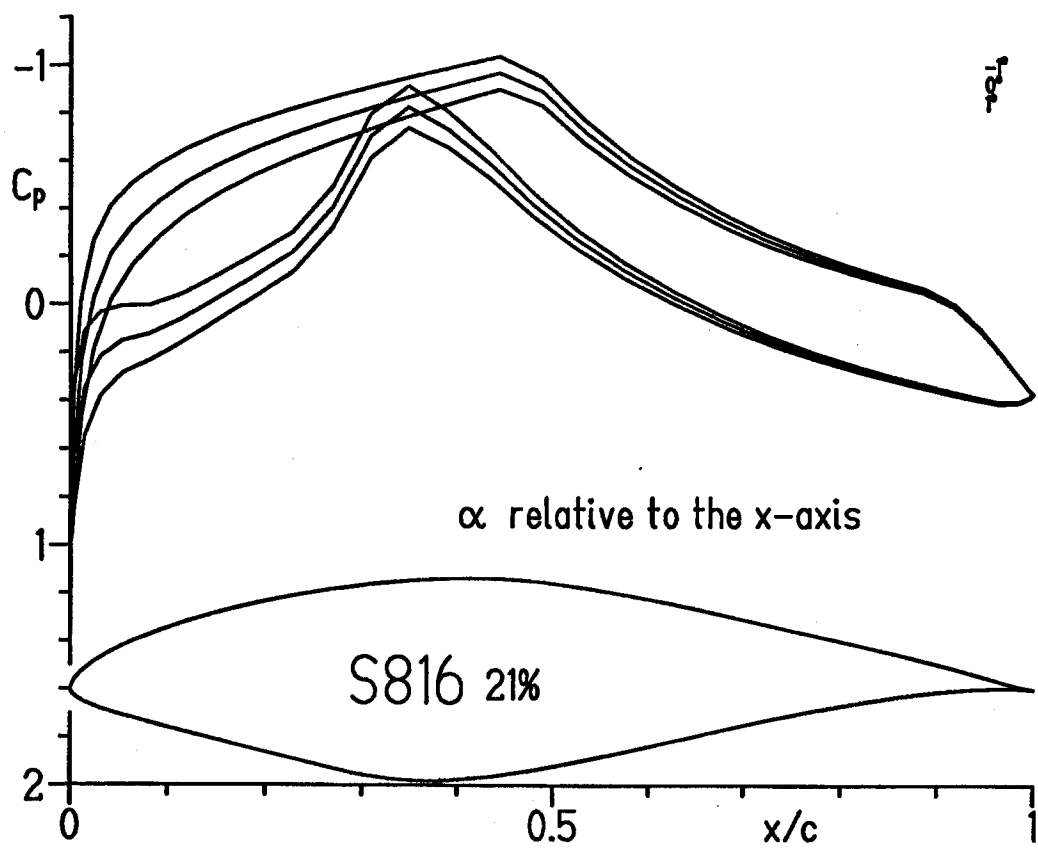
(c) S818.

Figure 1.- Airfoil shapes.



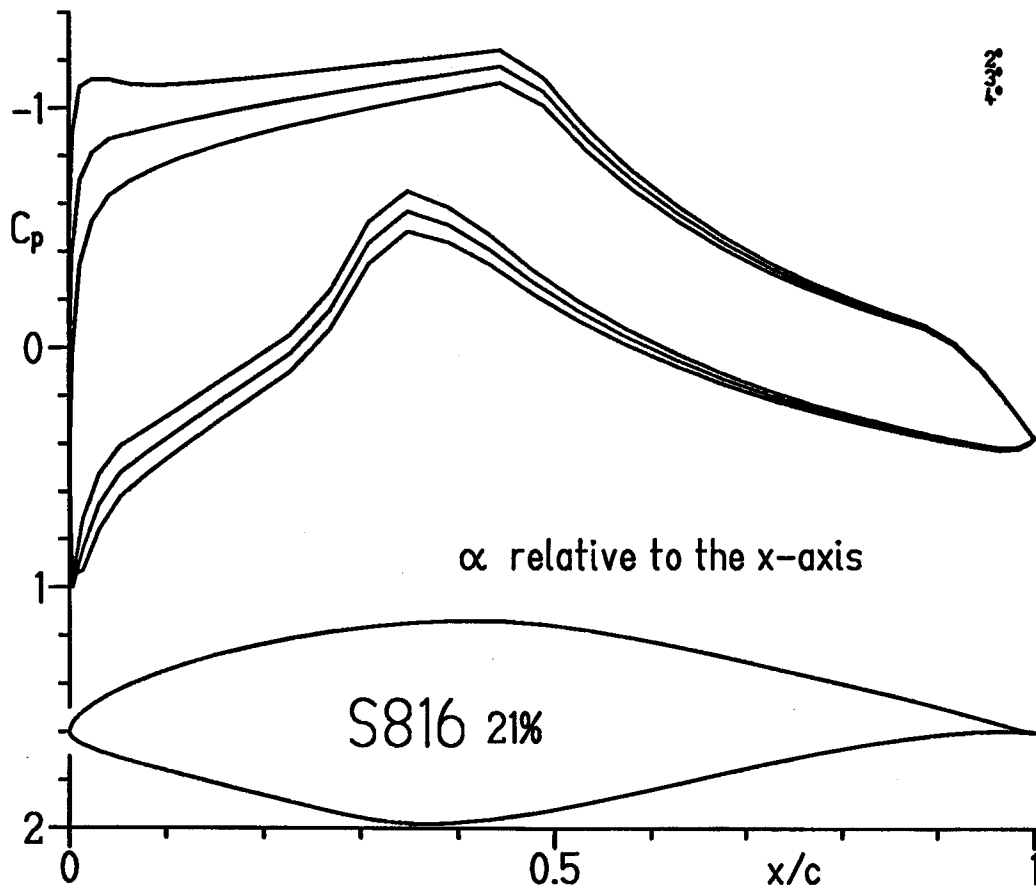
(a) $\alpha = -4^\circ, -3^\circ, \text{ and } -2^\circ$.

Figure 2.- Inviscid pressure distributions for S816 airfoil.



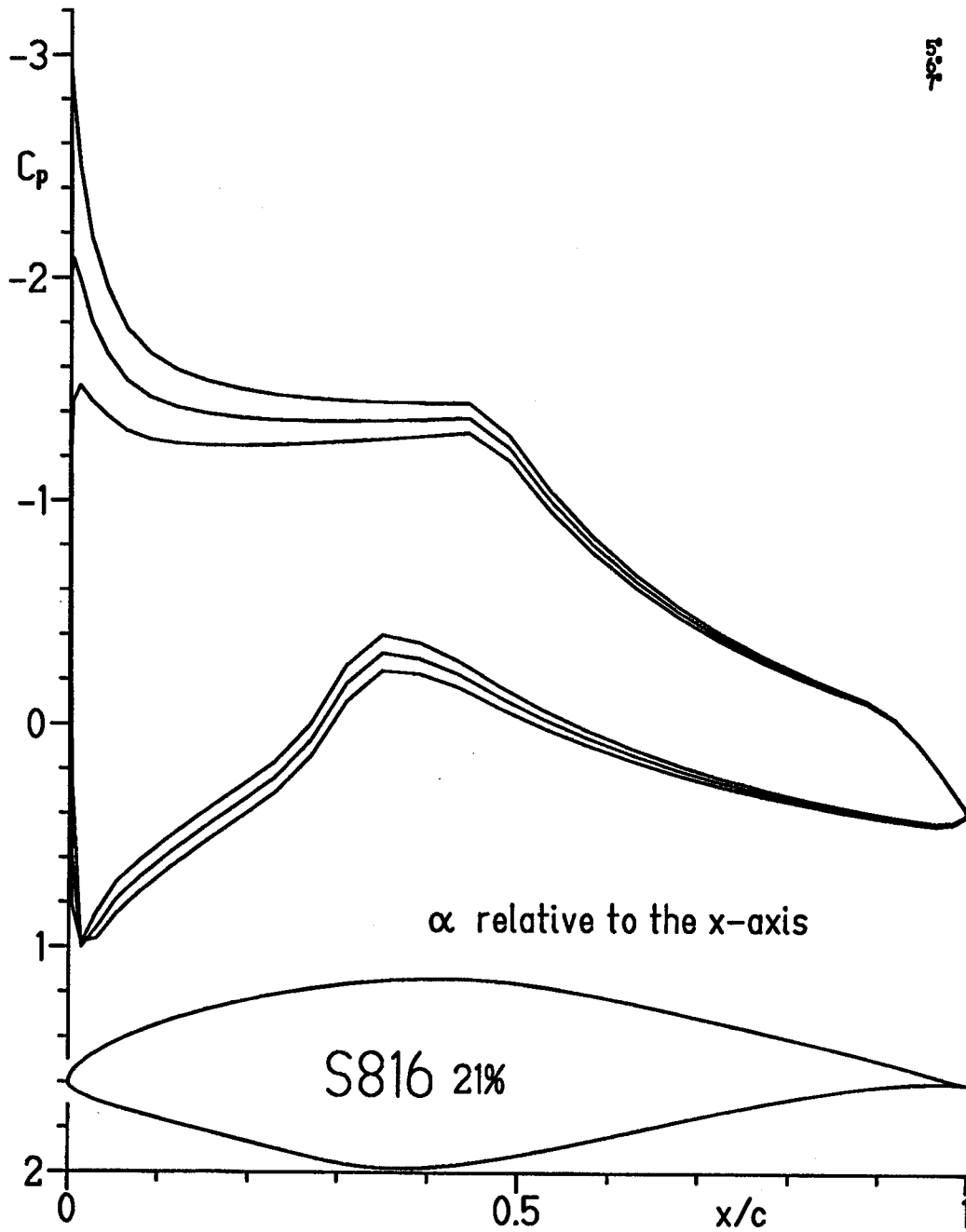
(b) $\alpha = -1^\circ, 0^\circ,$ and 1° .

Figure 2.- Continued.



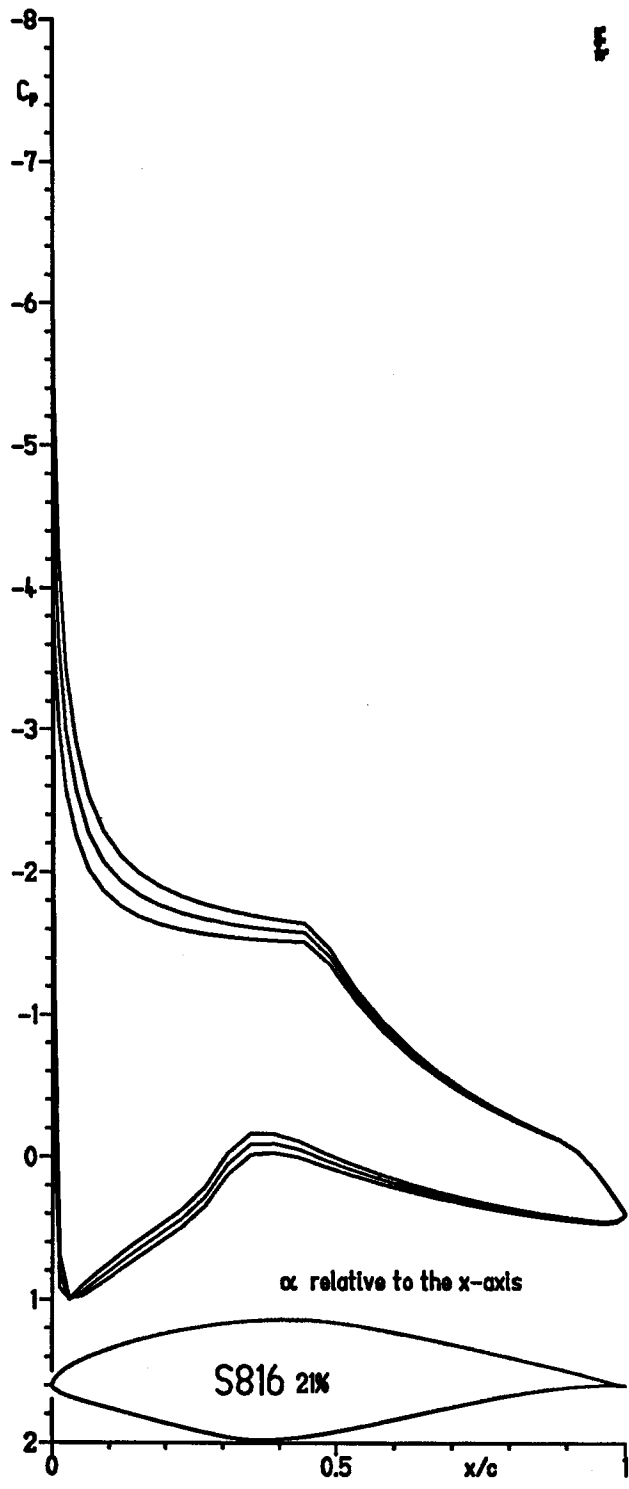
(c) $\alpha = 2^\circ, 3^\circ, \text{ and } 4^\circ$.

Figure 2.- Continued.



(d) $\alpha = 5^\circ, 6^\circ, \text{ and } 7^\circ$.

Figure 2.- Continued.



(e) $\alpha = 8^\circ, 9^\circ, \text{ and } 10^\circ$.

Figure 2.- Concluded.

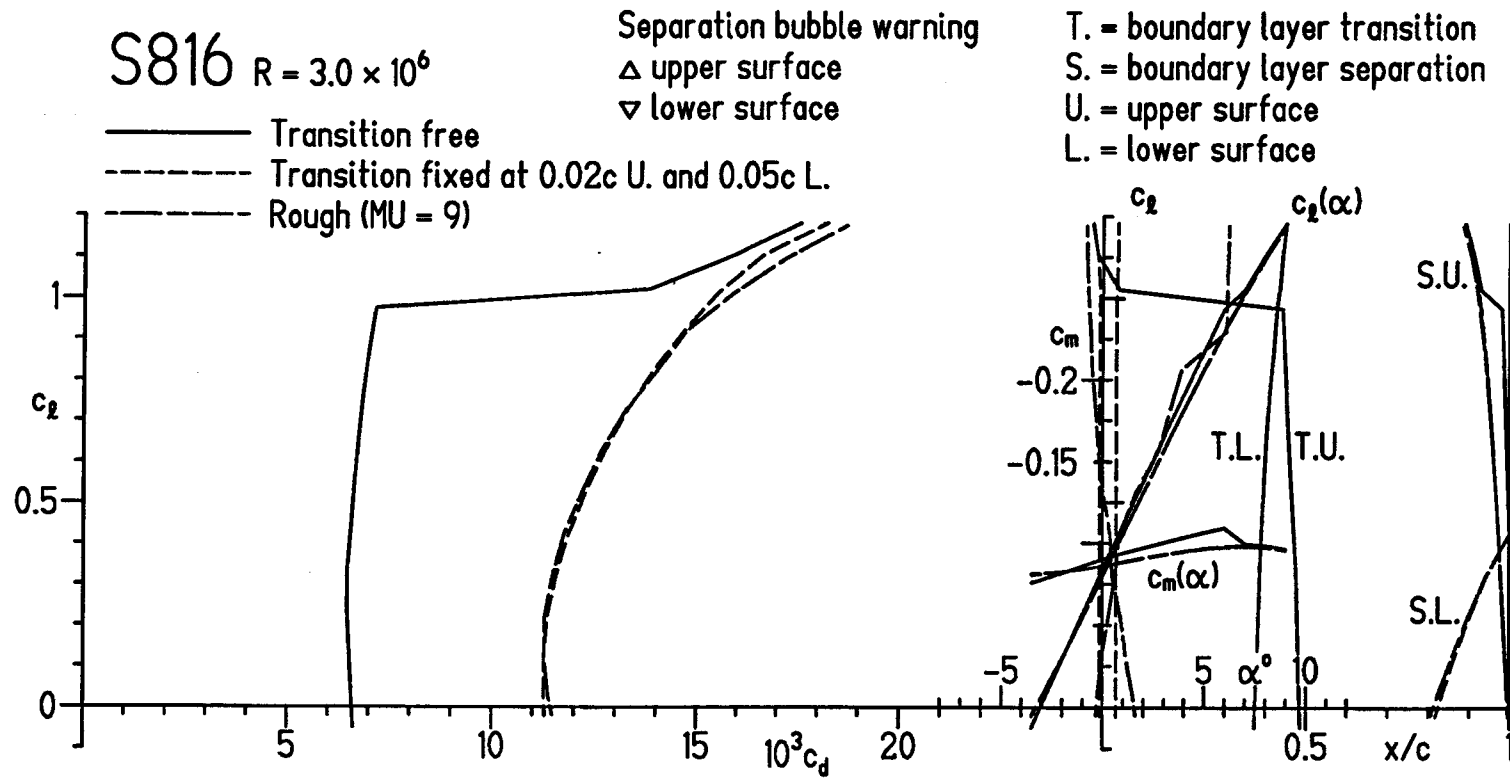
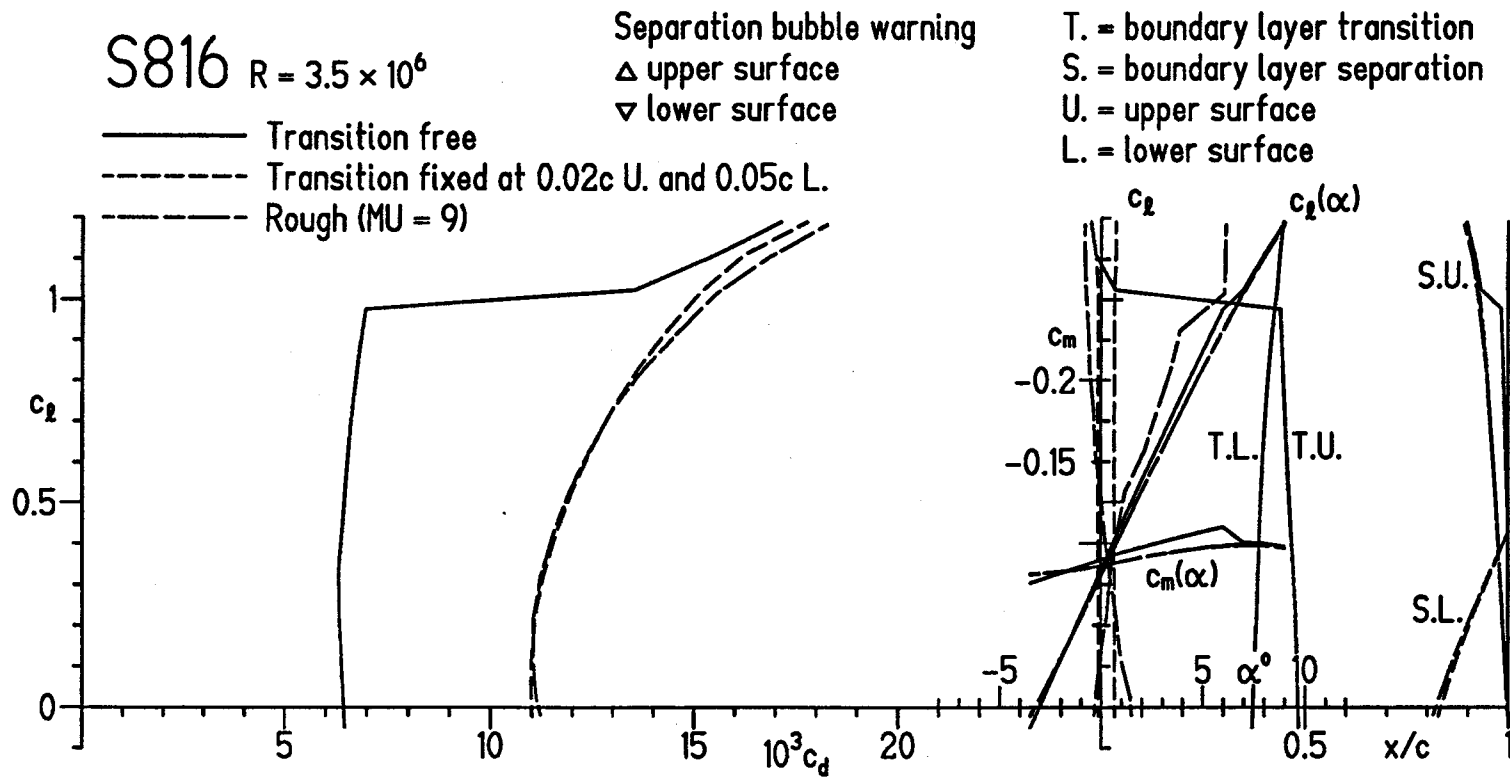
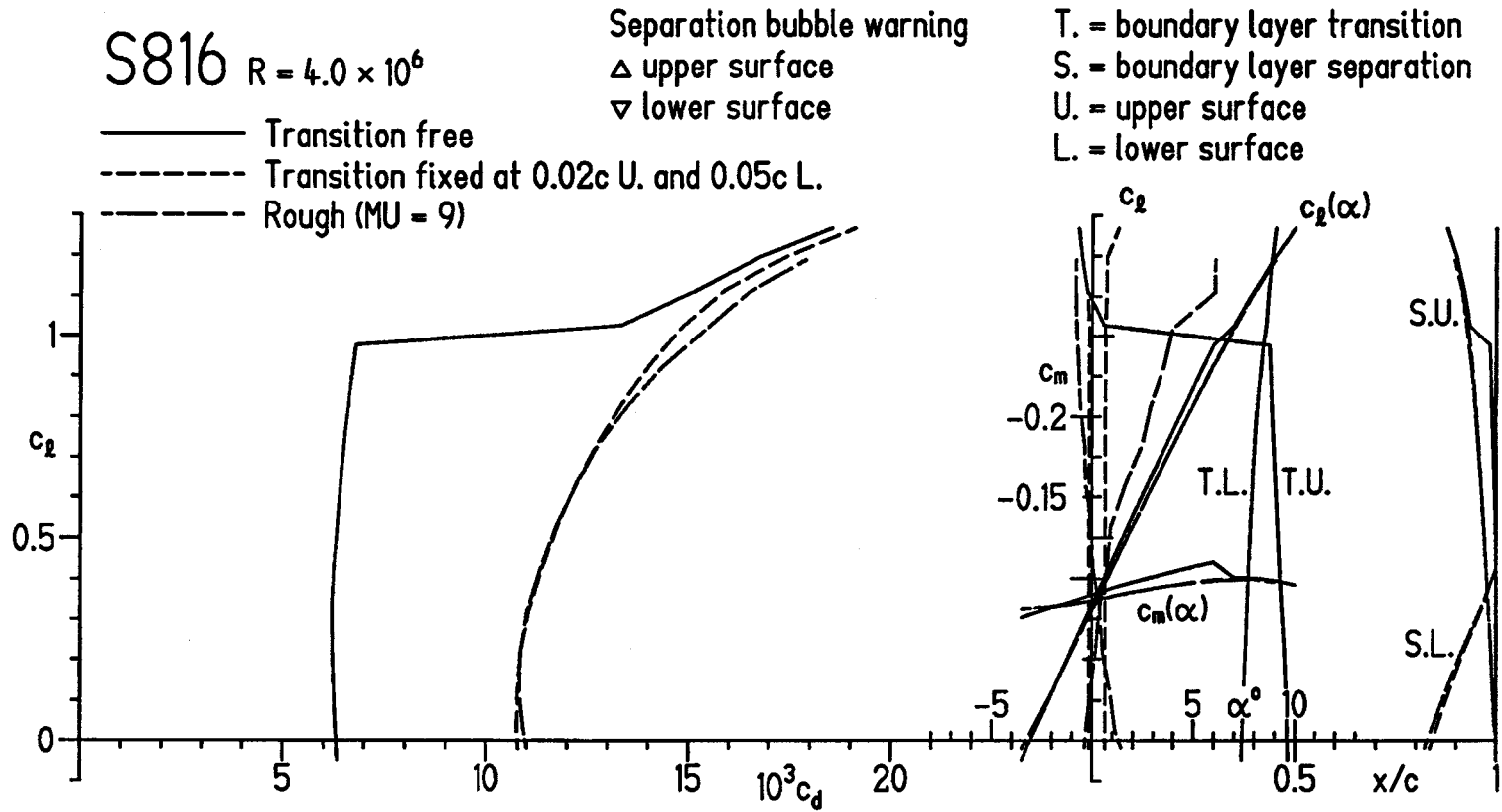


Figure 3.- Section characteristics of S816 airfoil with transition free and fixed and rough.



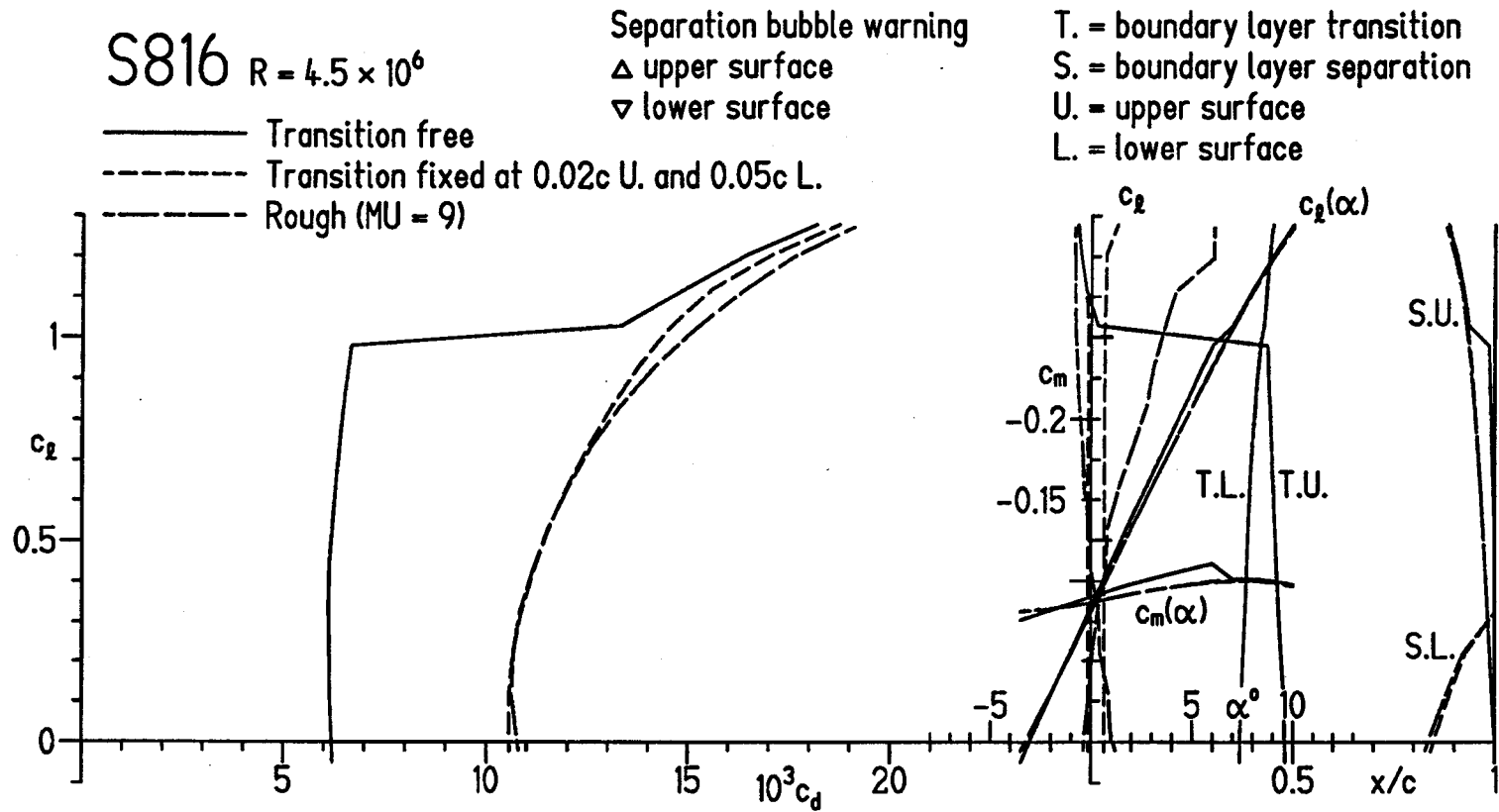
(b) $R = 3.5 \times 10^6$.

Figure 3.- Continued.



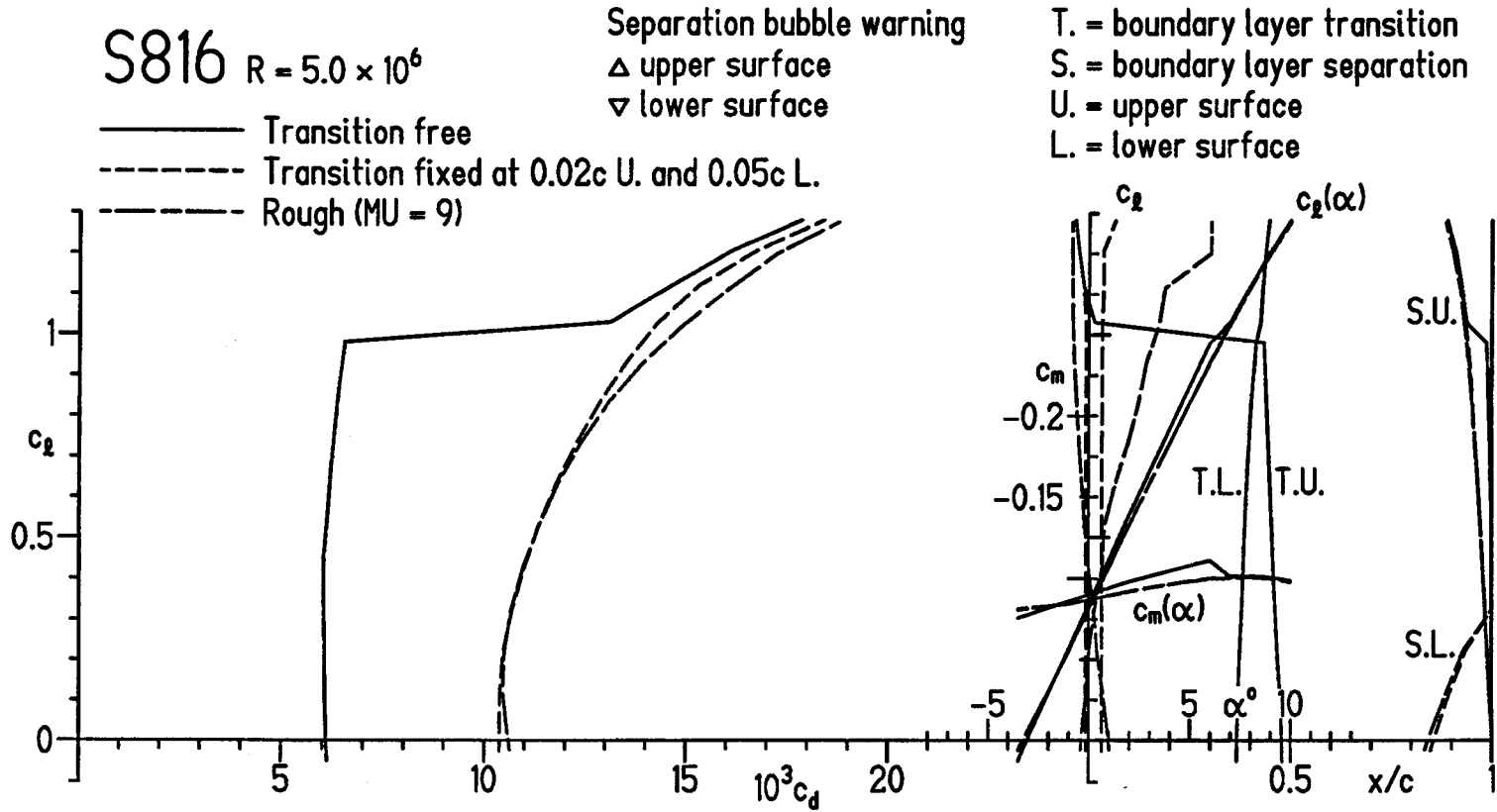
(c) $R = 4.0 \times 10^6$.

Figure 3.- Continued.



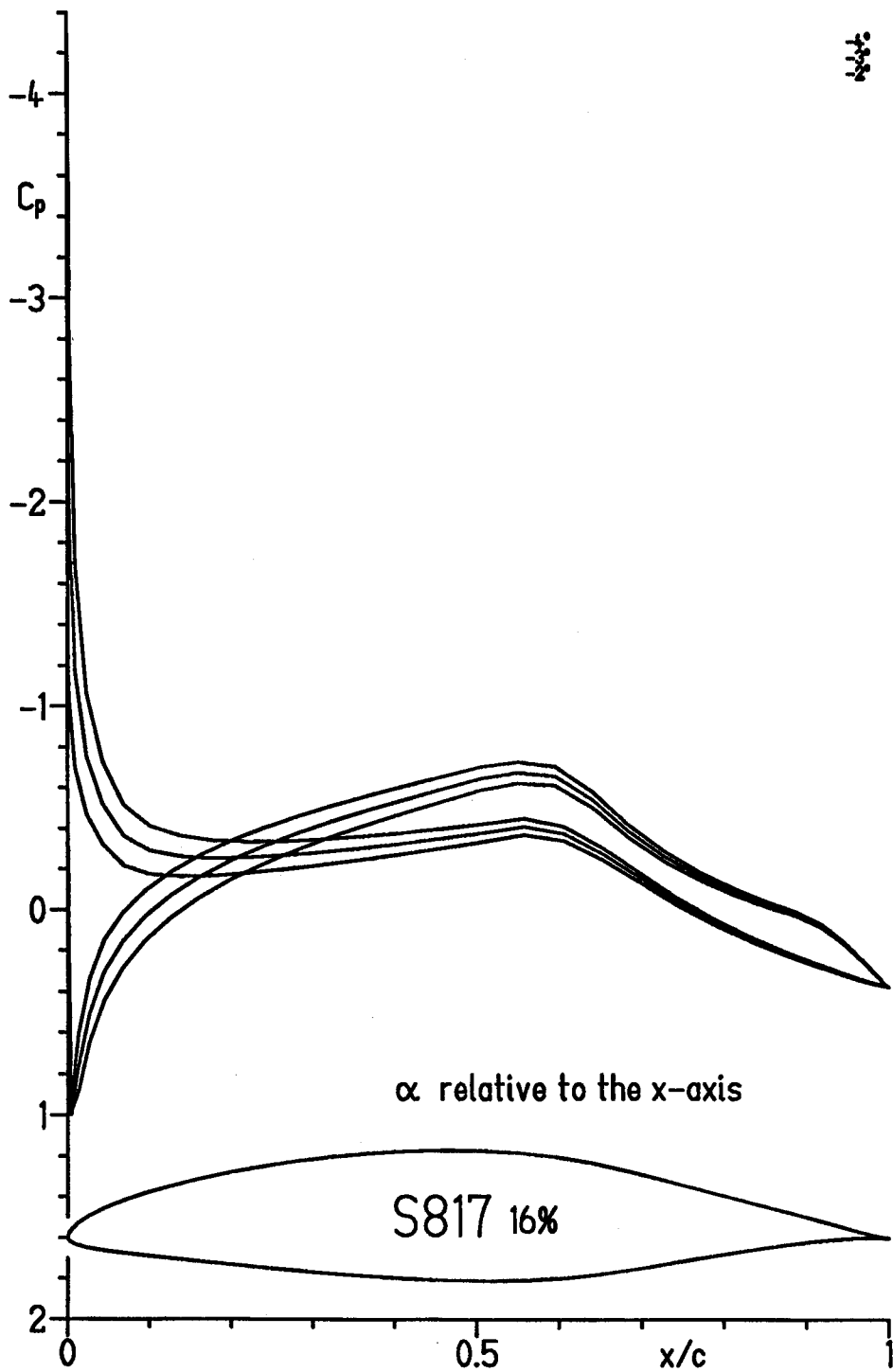
(d) $R = 4.5 \times 10^6$.

Figure 3.- Continued.



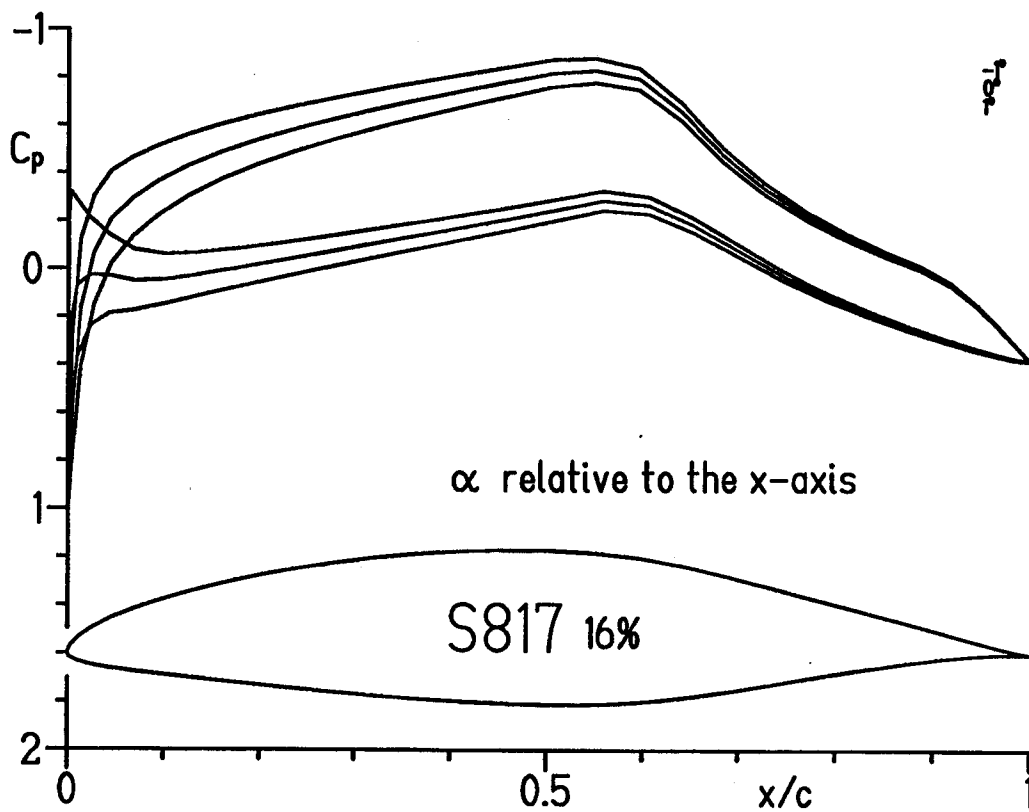
(e) $R = 5.0 \times 10^6$.

Figure 3.- Concluded.



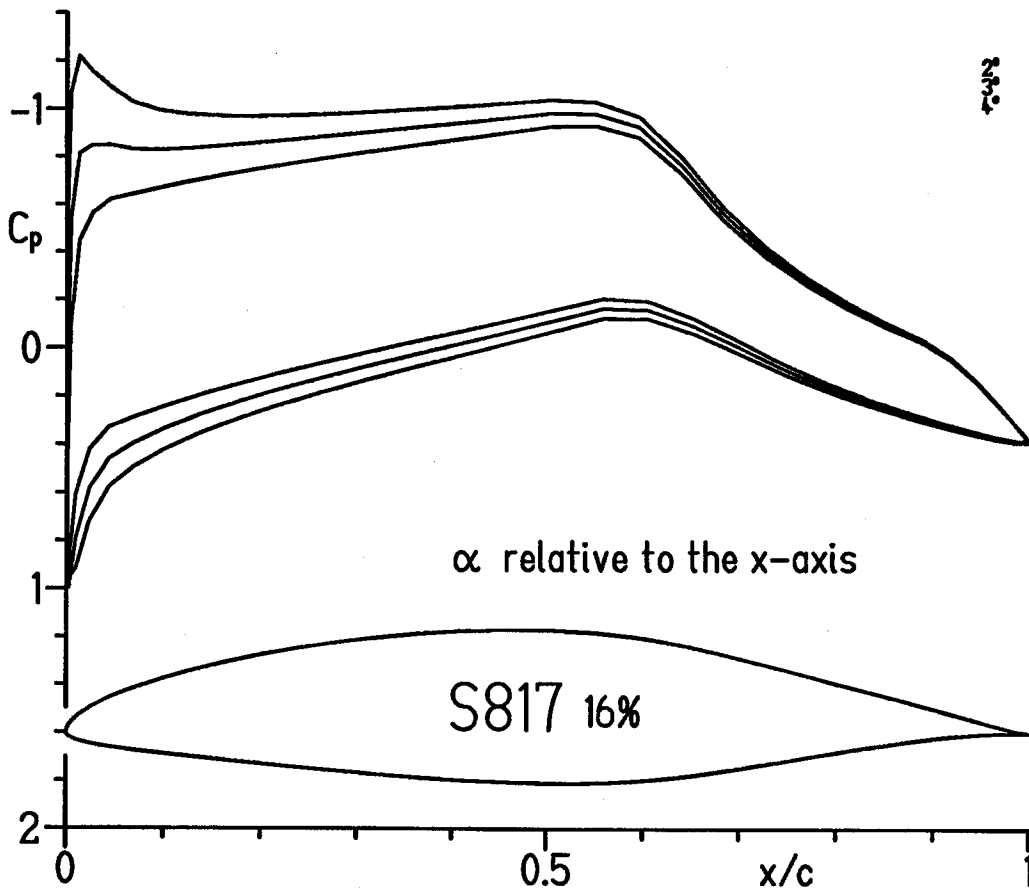
(a) $\alpha = -4^\circ, -3^\circ, \text{ and } -2^\circ$.

Figure 4.- Inviscid pressure distributions for S817 airfoil.



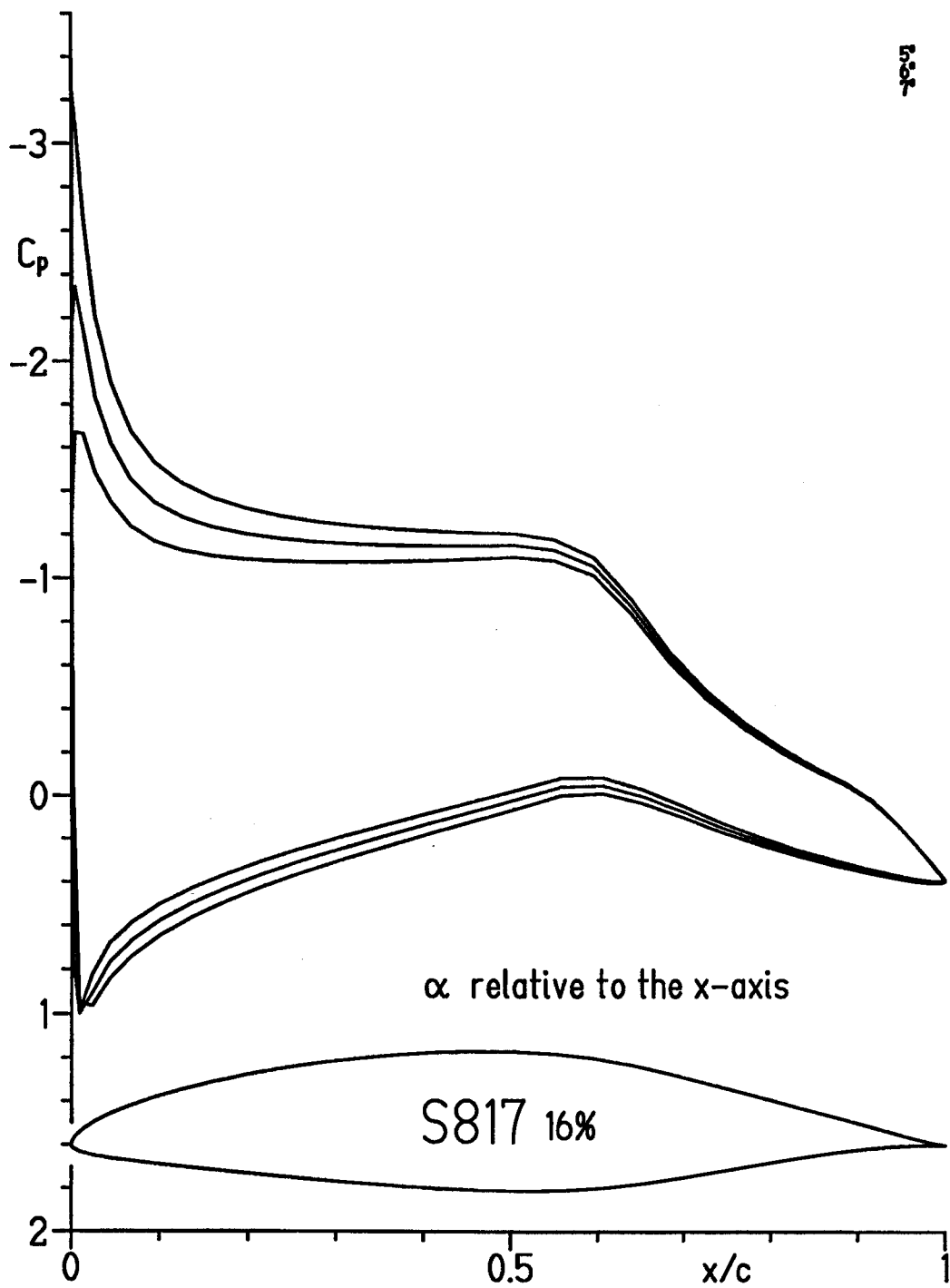
(b) $\alpha = -1^\circ, 0^\circ, \text{ and } 1^\circ$.

Figure 4.- Continued.



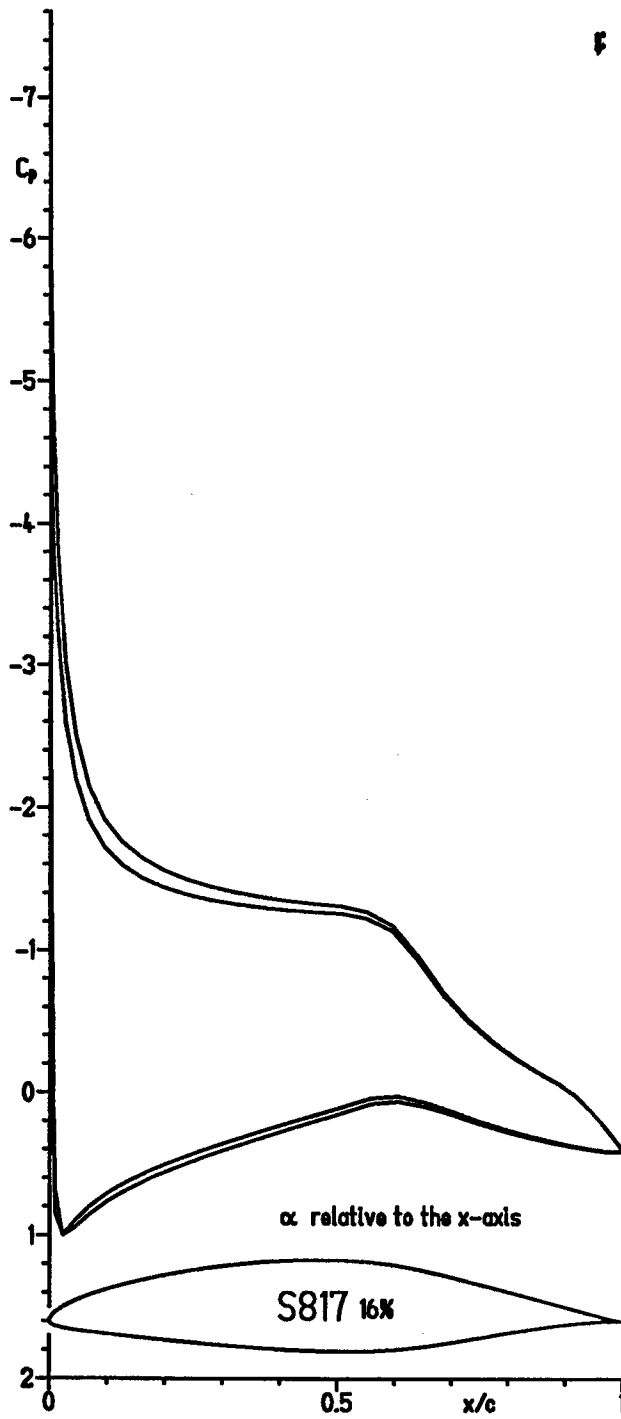
(c) $\alpha = 2^\circ, 3^\circ, \text{ and } 4^\circ$.

Figure 4.- Continued.



(d) $\alpha = 5^\circ, 6^\circ,$ and 7° .

Figure 4.- Continued.



(e) $\alpha = 8^\circ$ and 9° .

Figure 4.- Concluded.

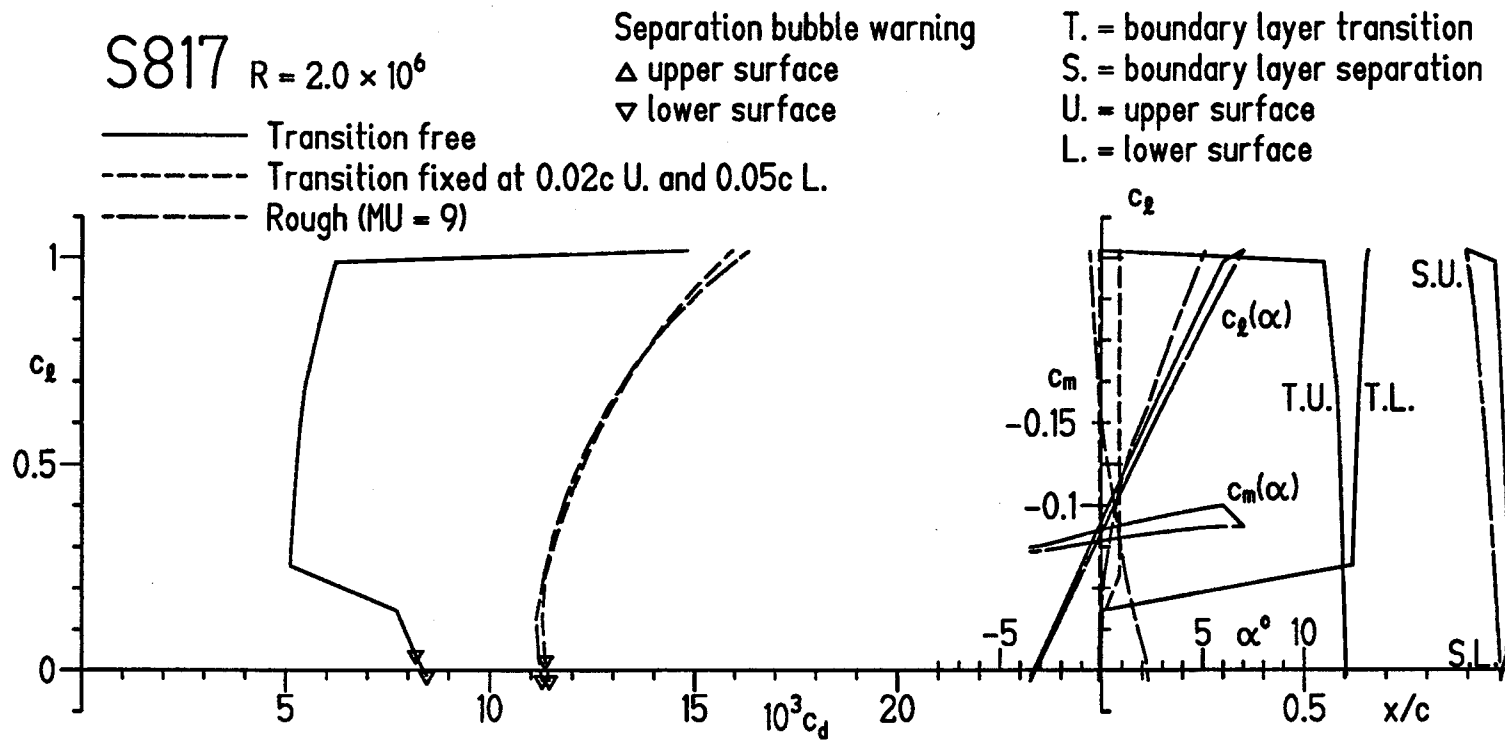
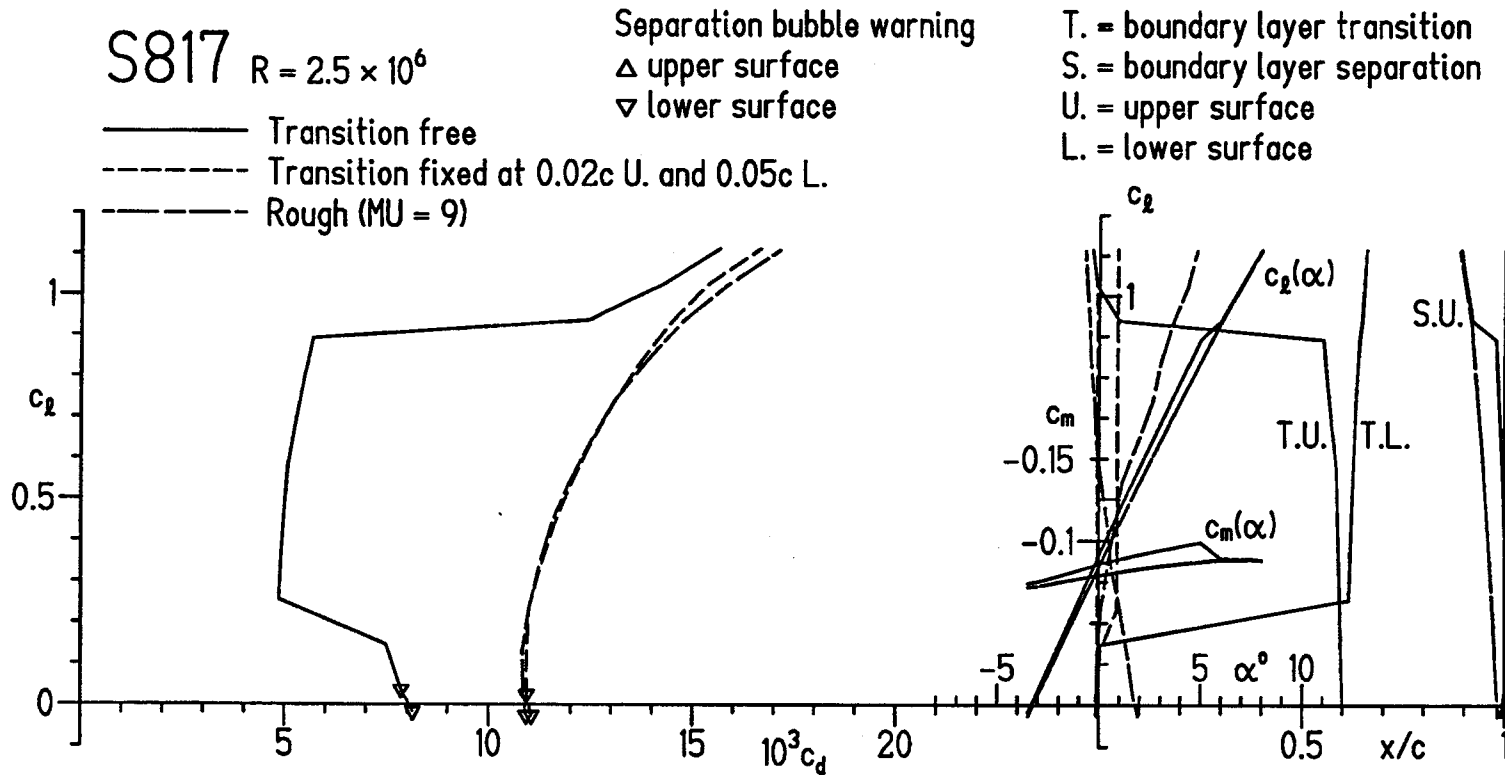
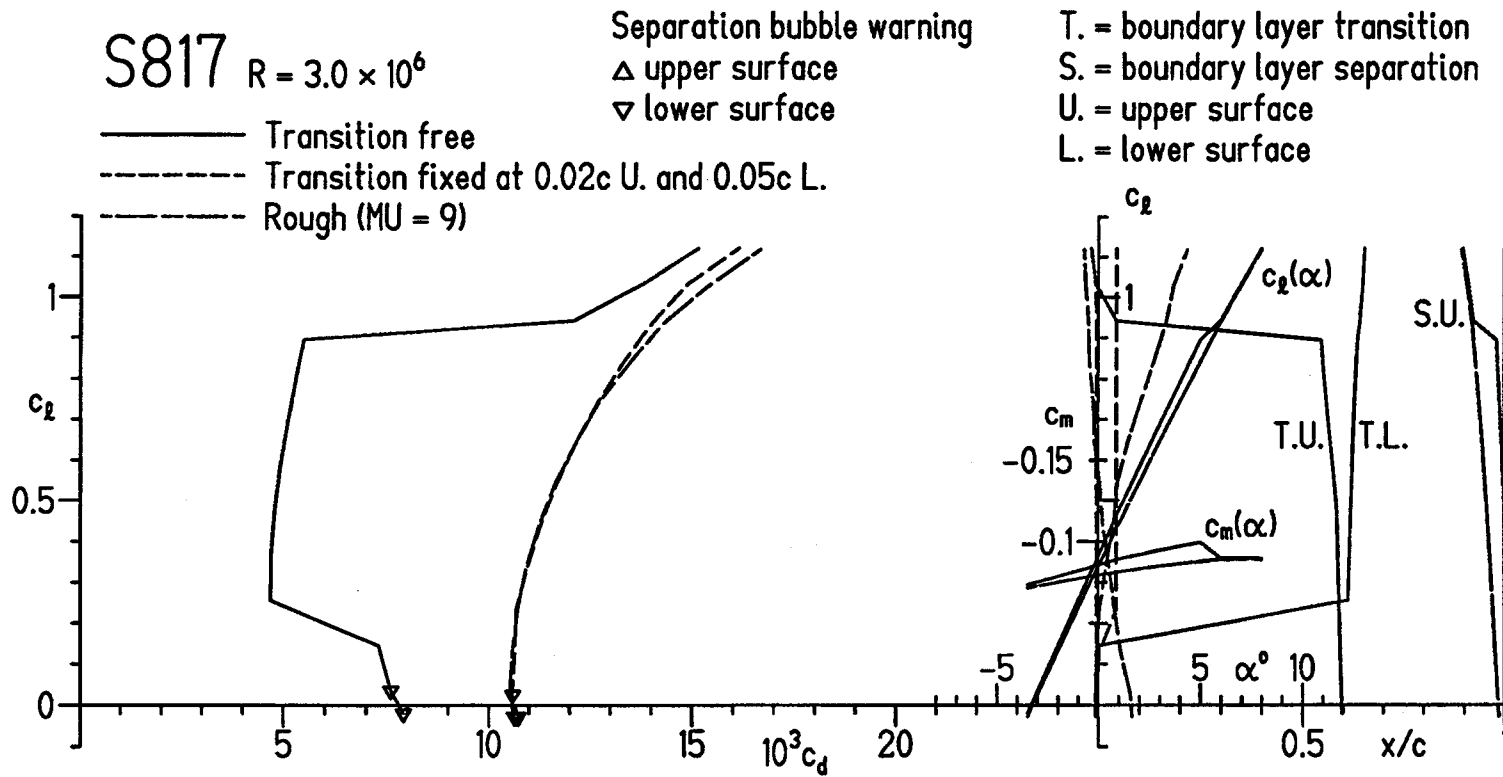
(a) $R = 2.0 \times 10^6$.

Figure 5.- Section characteristics of S817 airfoil with transition free and fixed and rough.



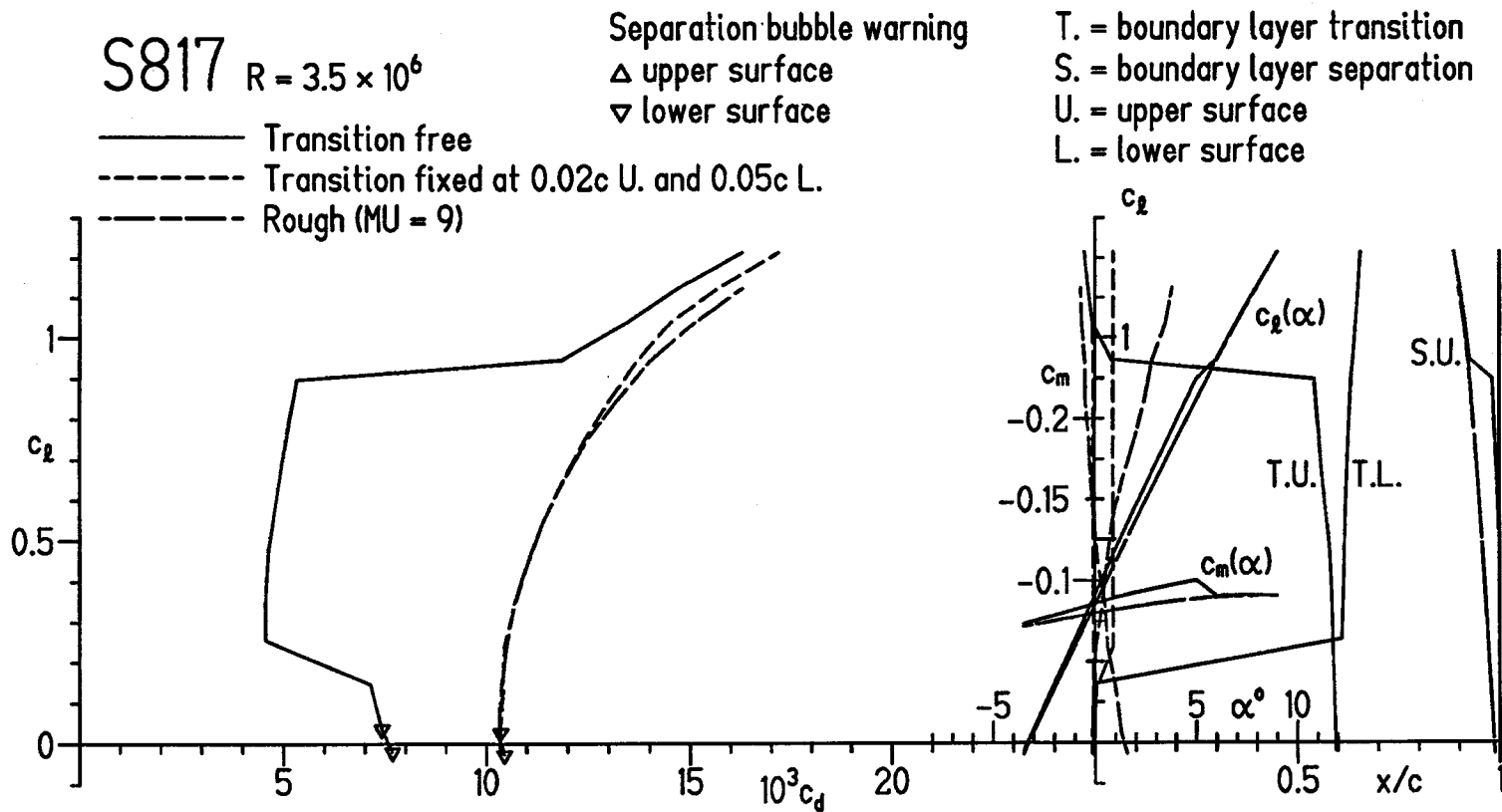
(b) $R = 2.5 \times 10^6$.

Figure 5.- Continued.



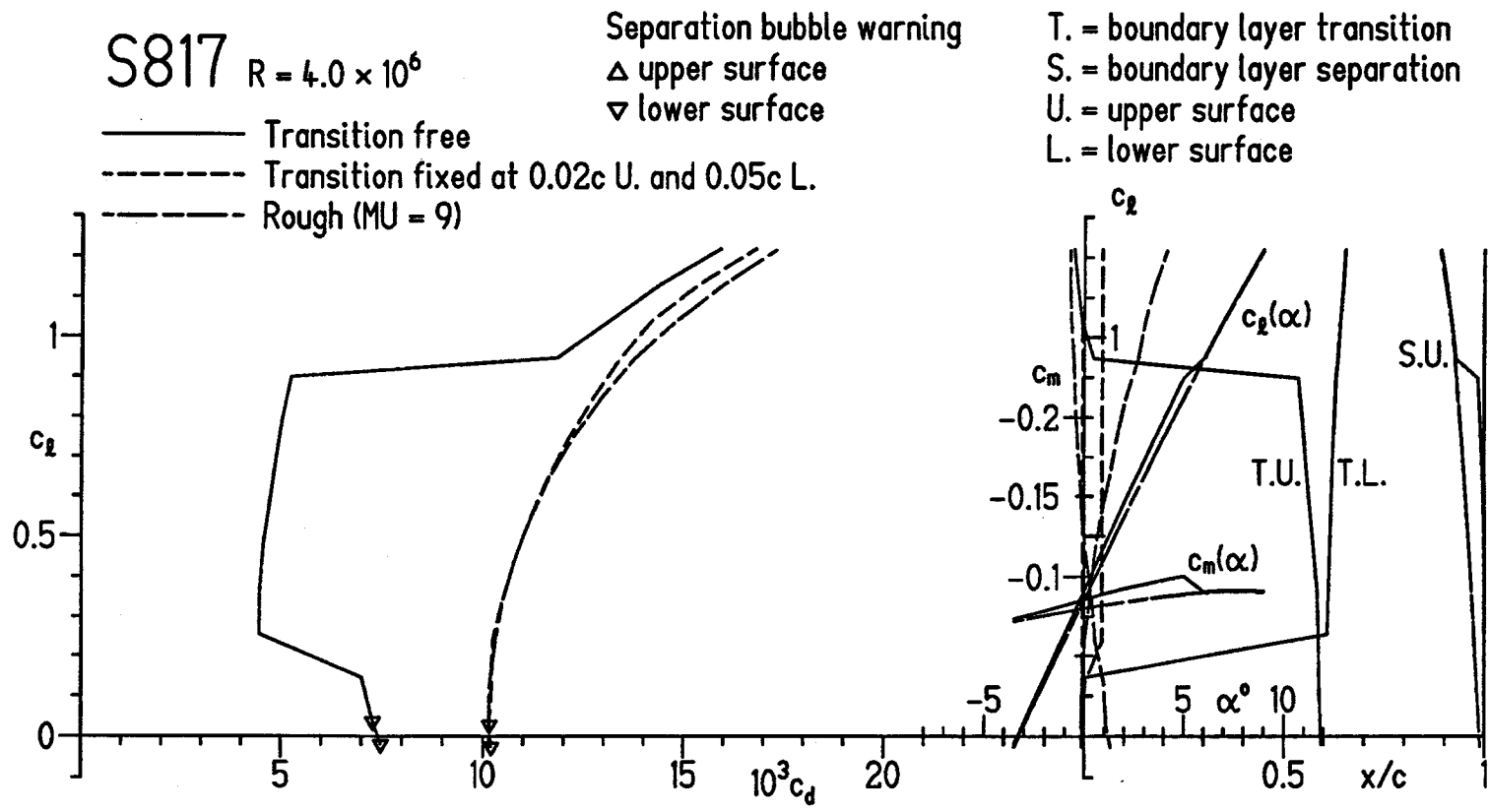
(c) $R = 3.0 \times 10^6$.

Figure 5.- Continued.



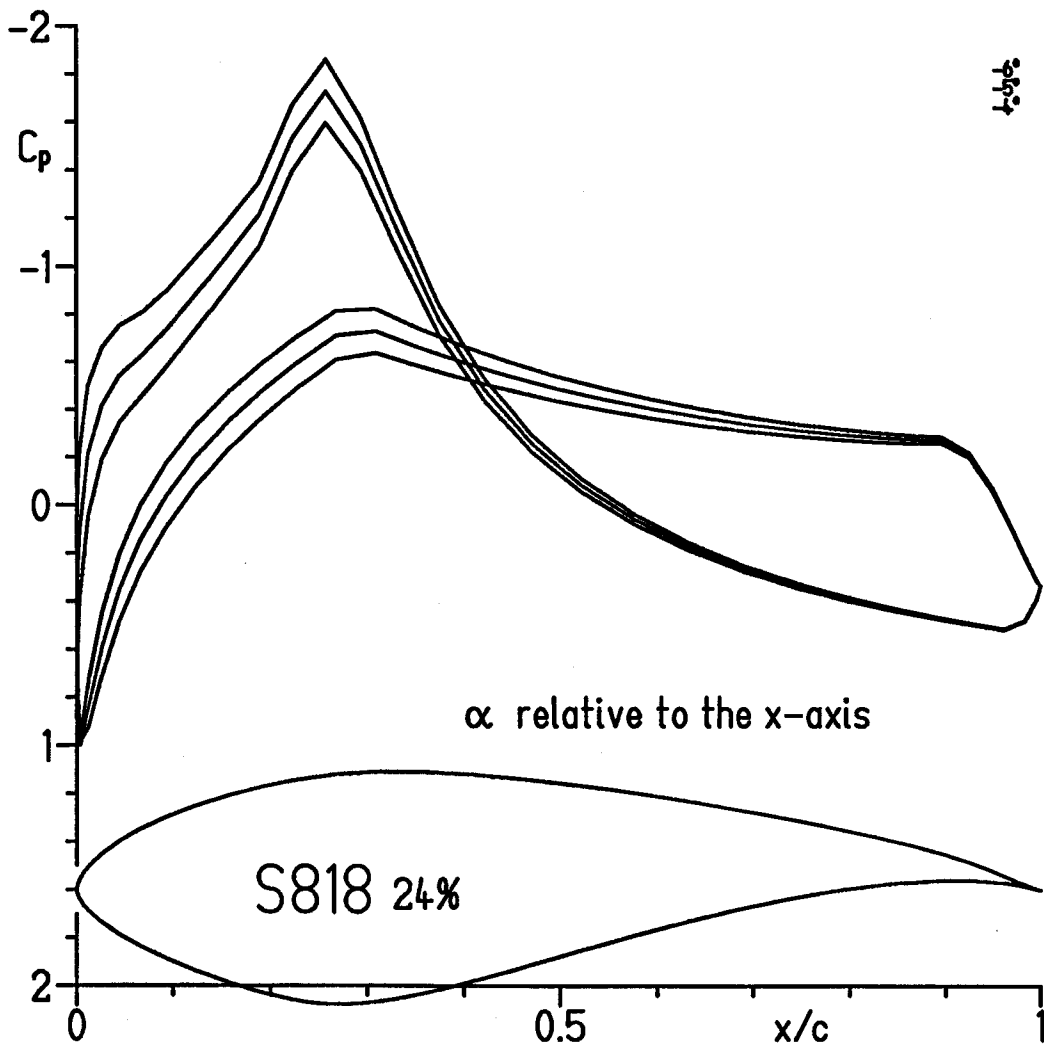
(d) $R = 3.5 \times 10^6$.

Figure 5.- Continued.



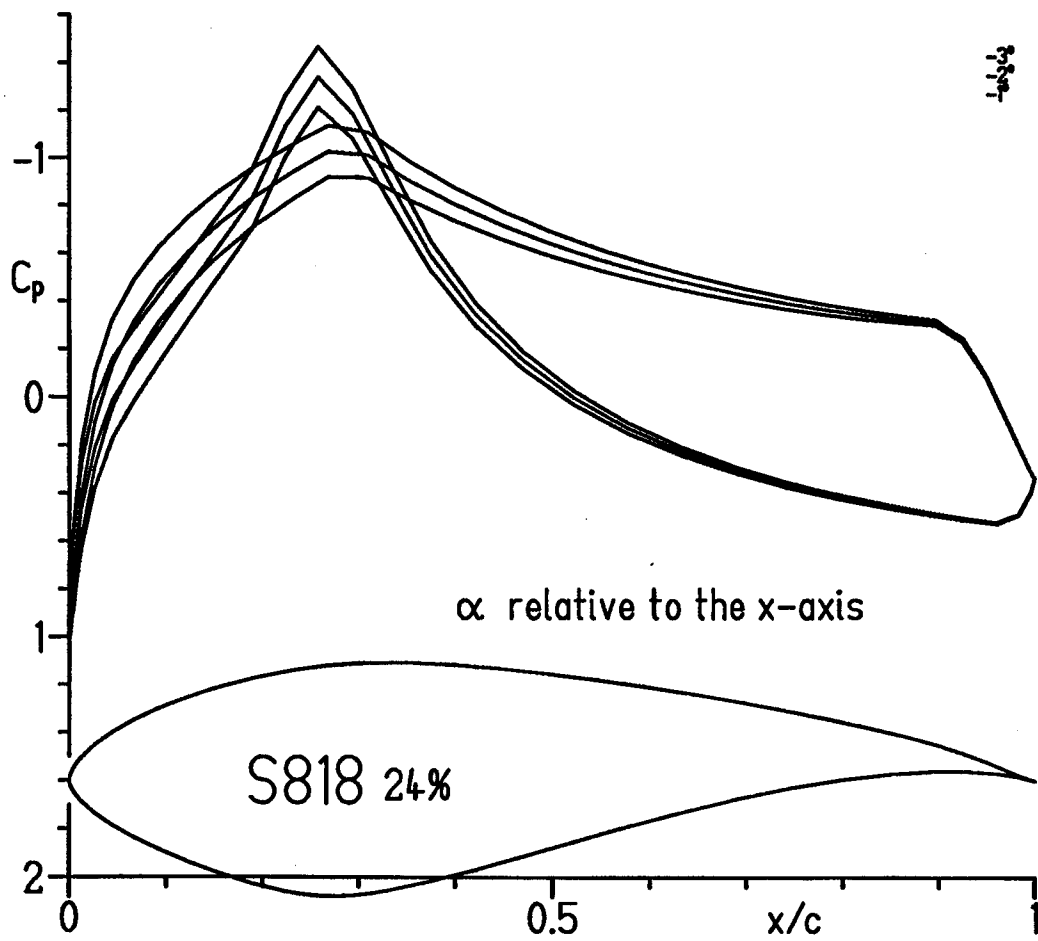
(e) $R = 4.0 \times 10^6$.

Figure 5.- Concluded.



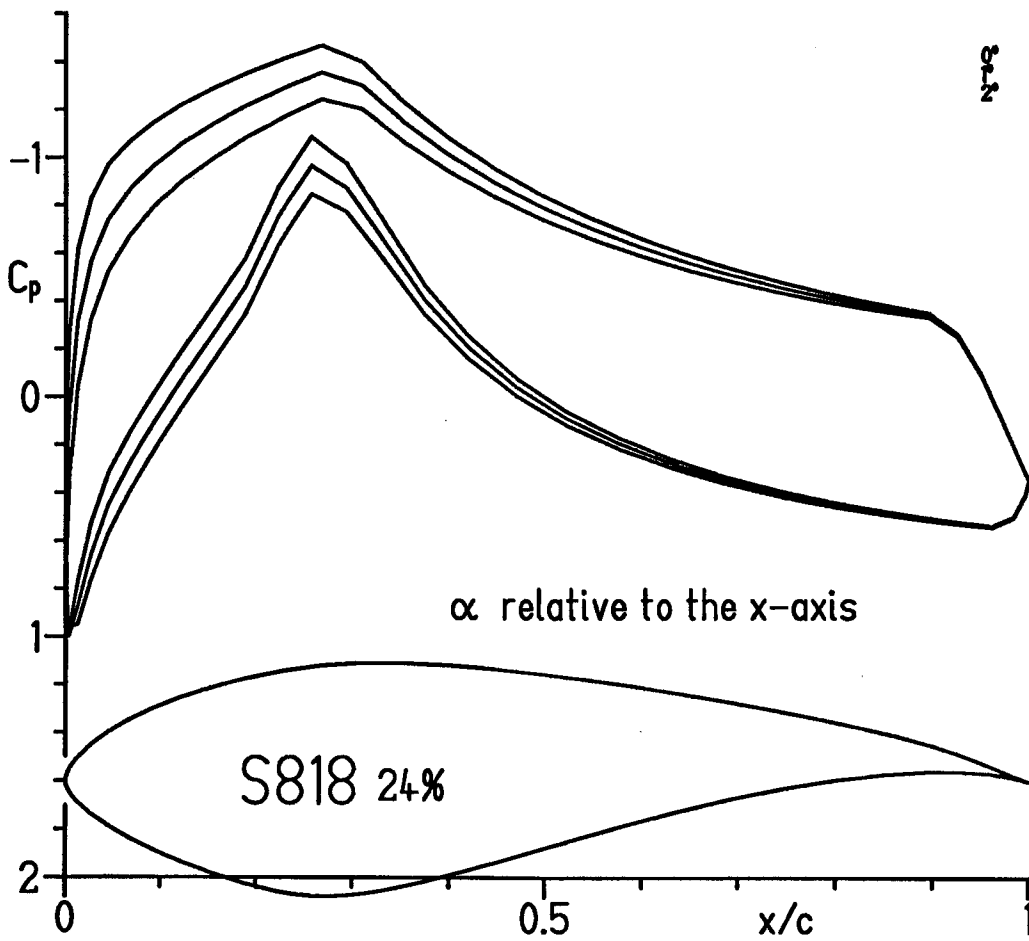
(a) $\alpha = -6^\circ, -5^\circ, \text{ and } -4^\circ$.

Figure 6.- Inviscid pressure distributions for S818 airfoil.



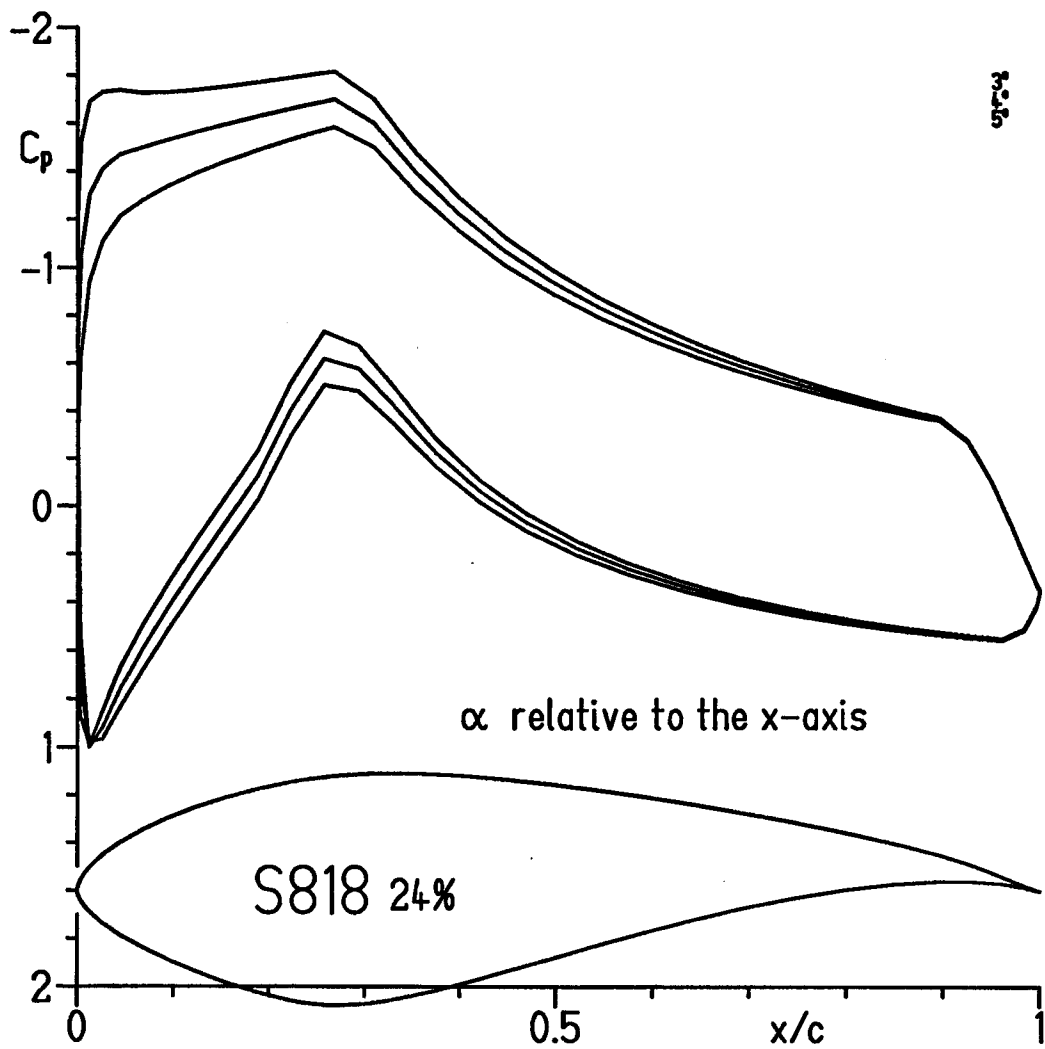
(b) $\alpha = -3^\circ, -2^\circ,$ and -1° .

Figure 6.- Continued.



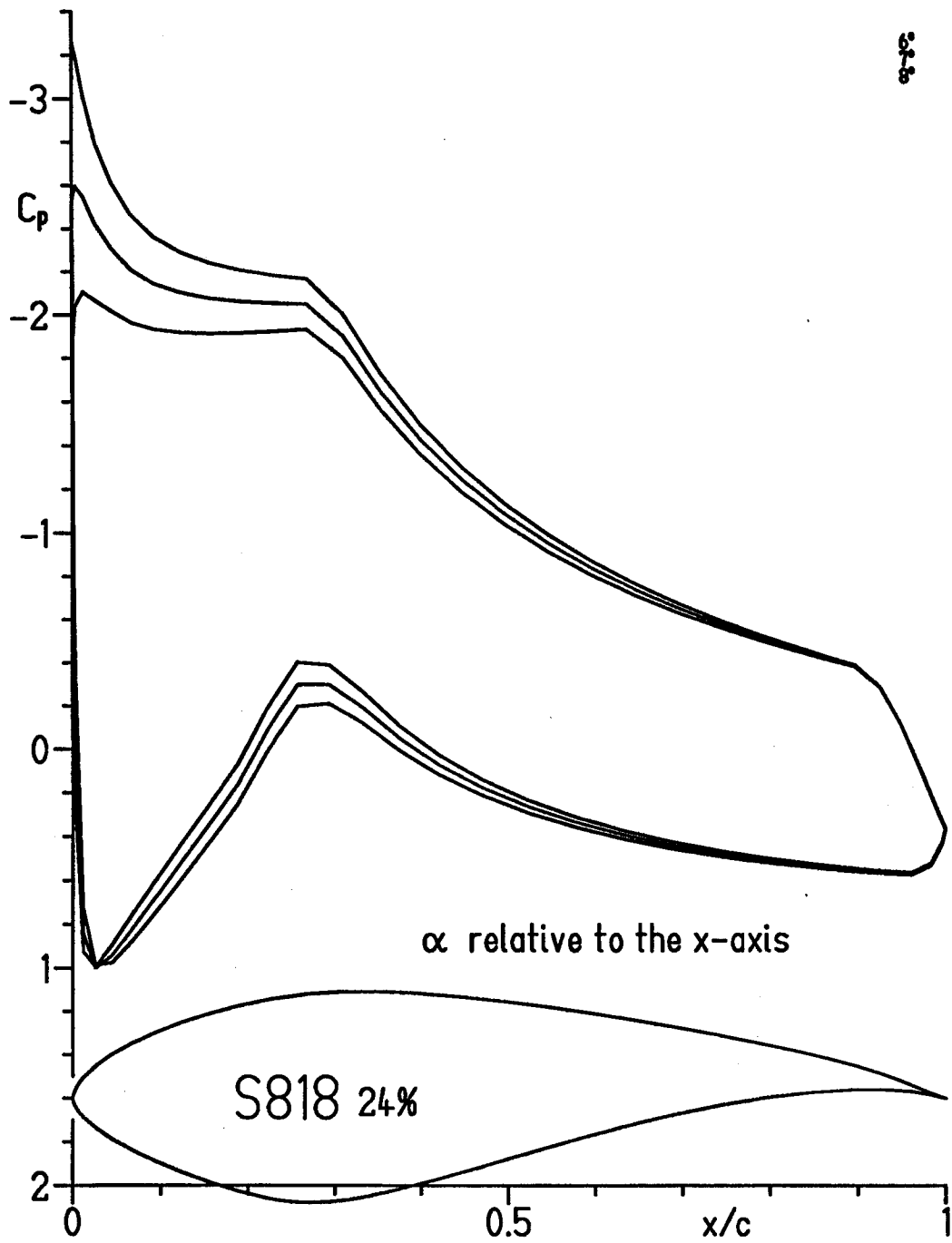
(c) $\alpha = 0^\circ, 1^\circ, \text{ and } 2^\circ$.

Figure 6.- Continued.



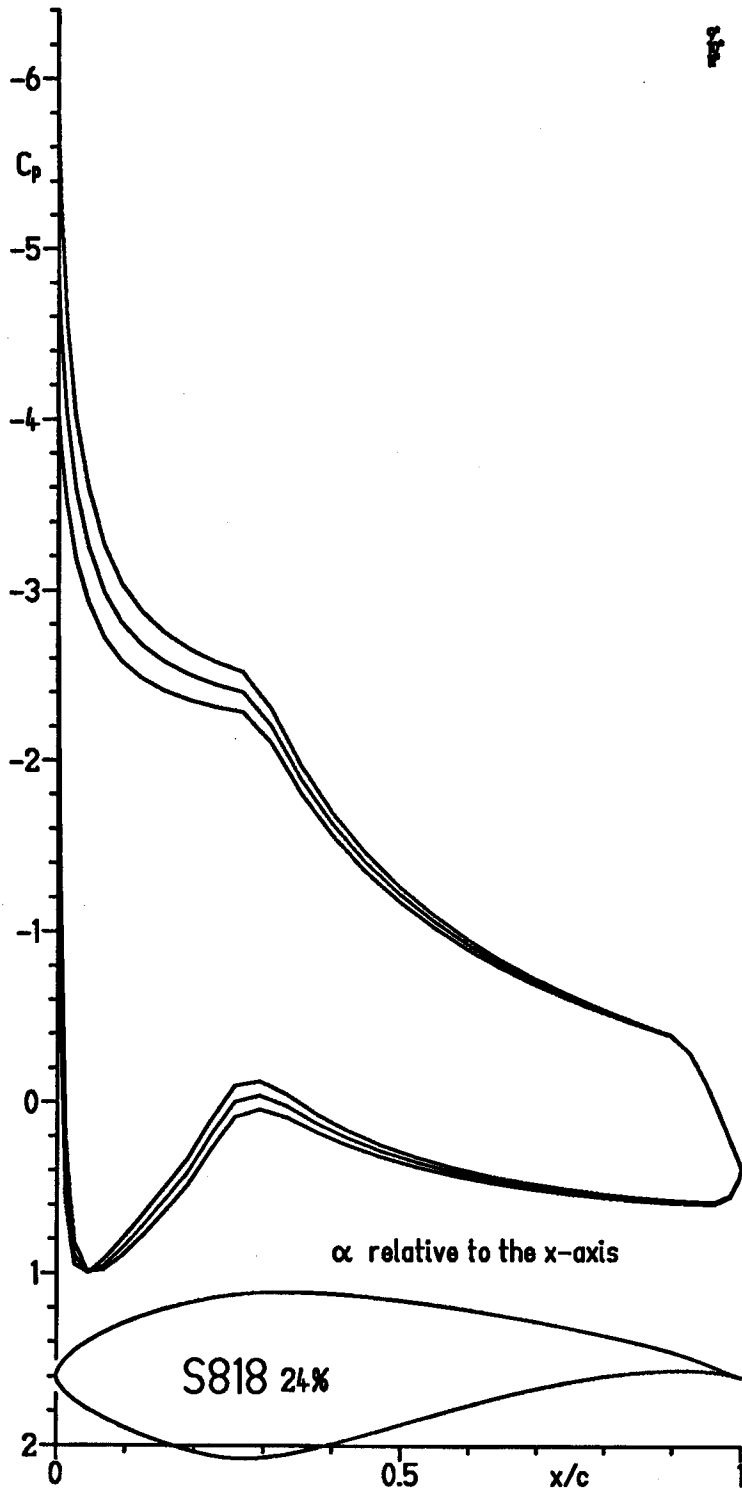
(d) $\alpha = 3^\circ, 4^\circ, \text{ and } 5^\circ$.

Figure 6.- Continued.



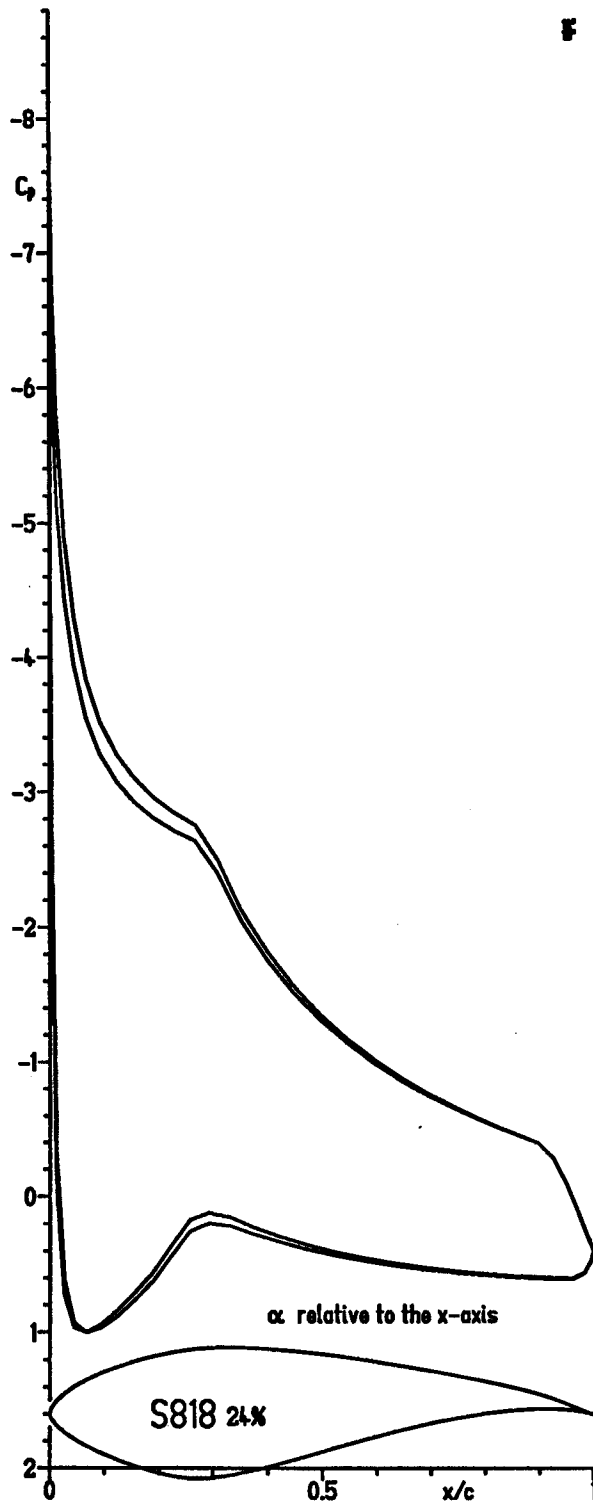
(e) $\alpha = 6^\circ, 7^\circ, \text{ and } 8^\circ$.

Figure 6.- Continued.



(f) $\alpha = 9^\circ, 10^\circ, \text{ and } 11^\circ$.

Figure 6.- Continued.



(g) $\alpha = 12^\circ$ and 13° .

Figure 6.- Concluded.

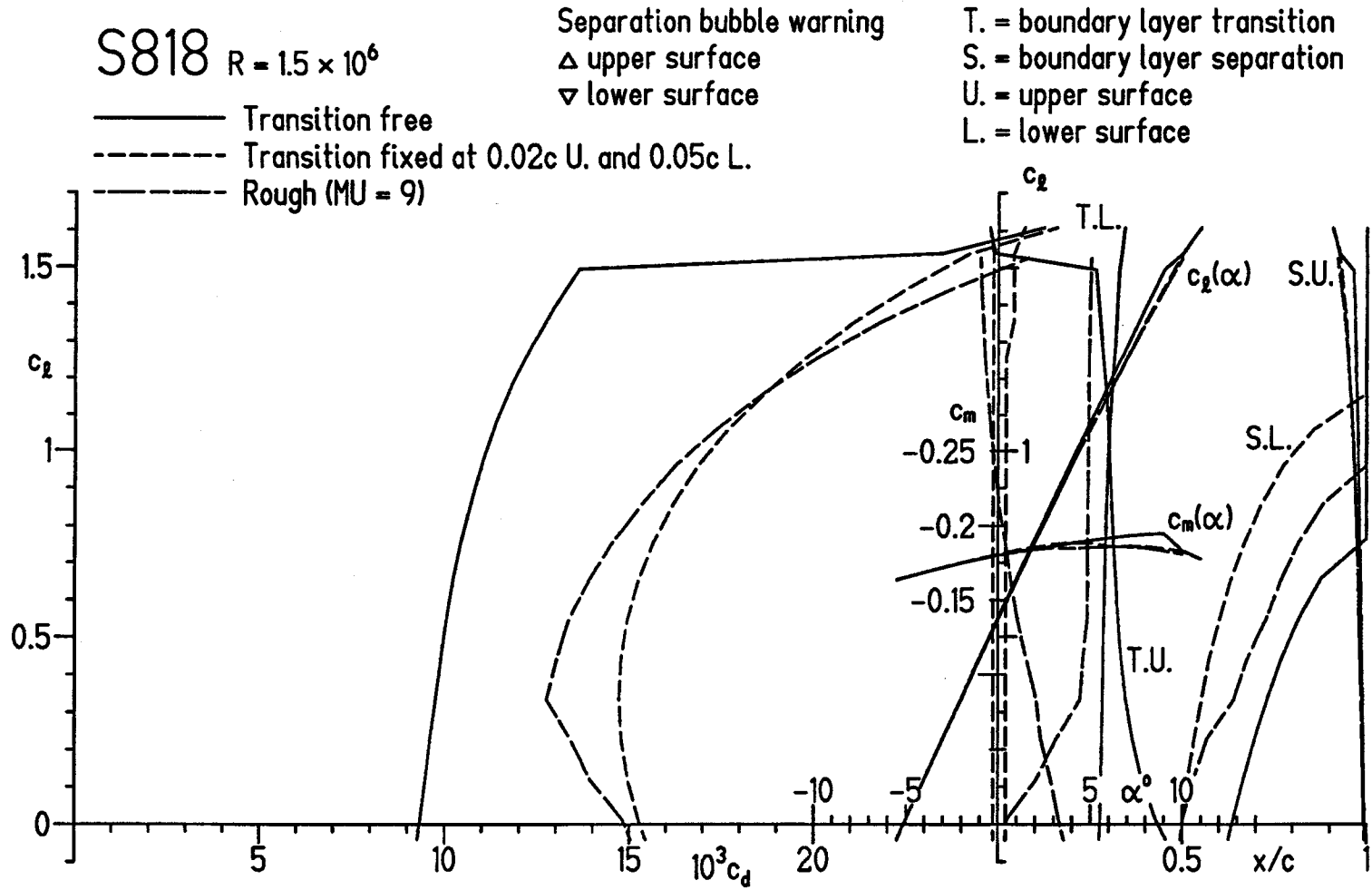
(a) $R = 1.5 \times 10^6$.

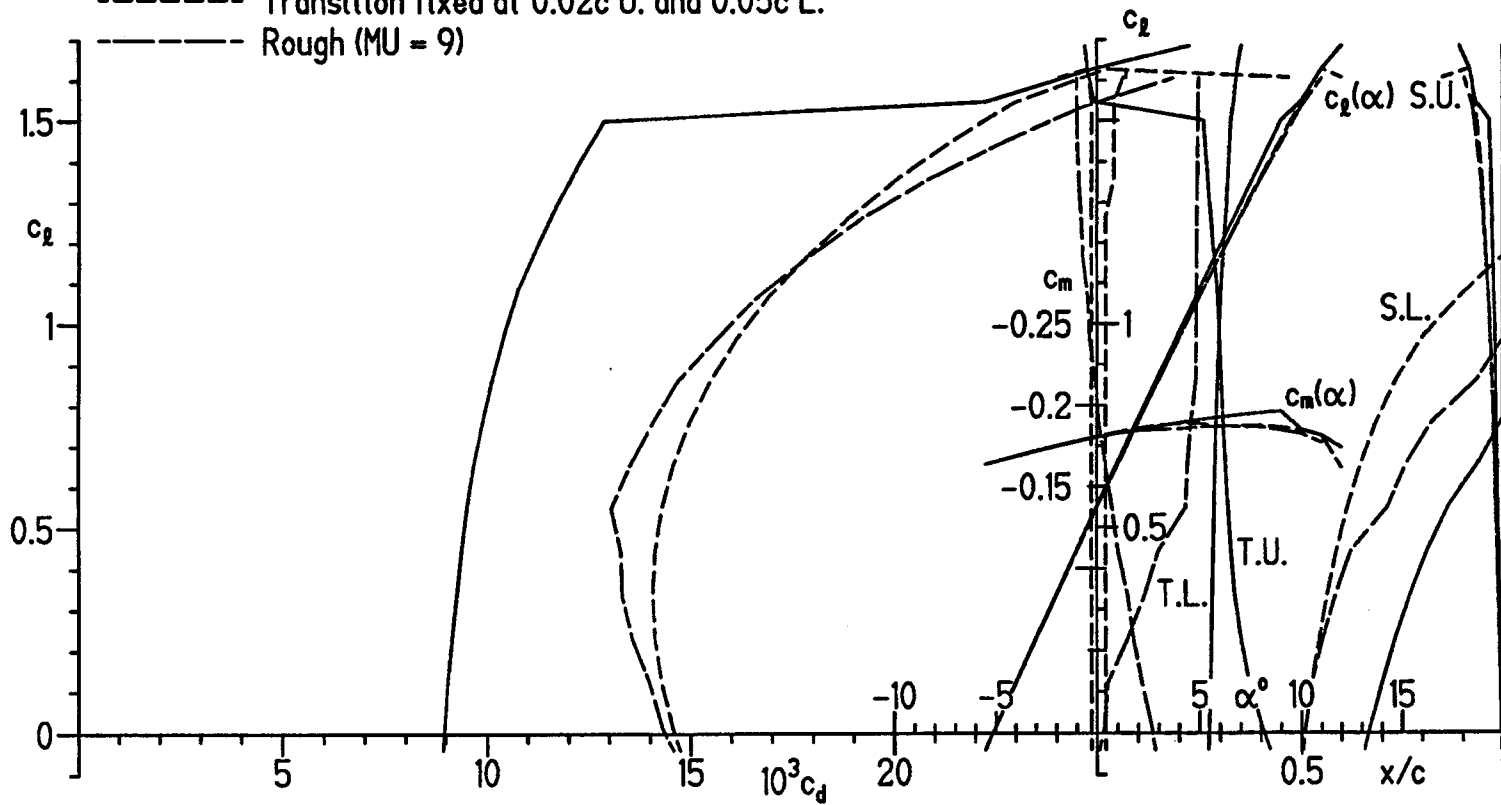
Figure 7.- Section characteristics of S818 airfoil with transition free and fixed and rough.

S818 $R = 2.0 \times 10^6$

- Transition free
- - - Transition fixed at $0.02c$ U. and $0.05c$ L.
- · - · - Rough ($MU = 9$)

Separation bubble warning
 Δ upper surface
 ∇ lower surface

T. = boundary layer transition
 S. = boundary layer separation
 U. = upper surface
 L. = lower surface



(b) $R = 2.0 \times 10^6$.

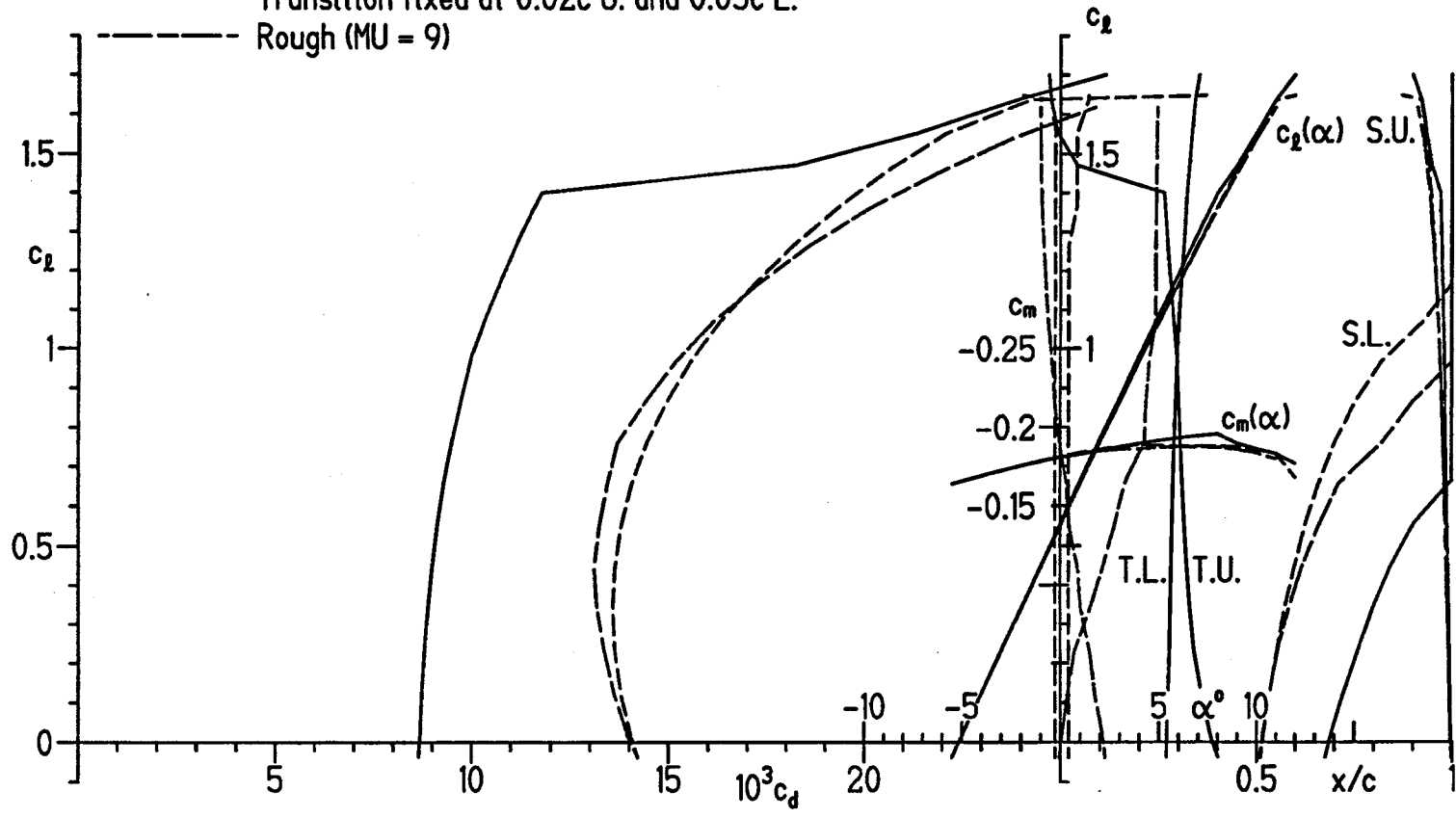
Figure 7.- Continued.

S818 $R = 2.5 \times 10^6$

Separation bubble warning
 Δ upper surface
 ∇ lower surface

T. = boundary layer transition
 S. = boundary layer separation
 U. = upper surface
 L. = lower surface

— Transition free
 - - - Transition fixed at $0.02c_U$ and $0.05c_L$.
 - - - Rough ($MU = 9$)



(c) $R = 2.5 \times 10^6$.

Figure 7.- Continued.

S818 $R = 3.0 \times 10^6$

Separation bubble warning

Δ upper surface

∇ lower surface

T. = boundary layer transition

S. = boundary layer separation

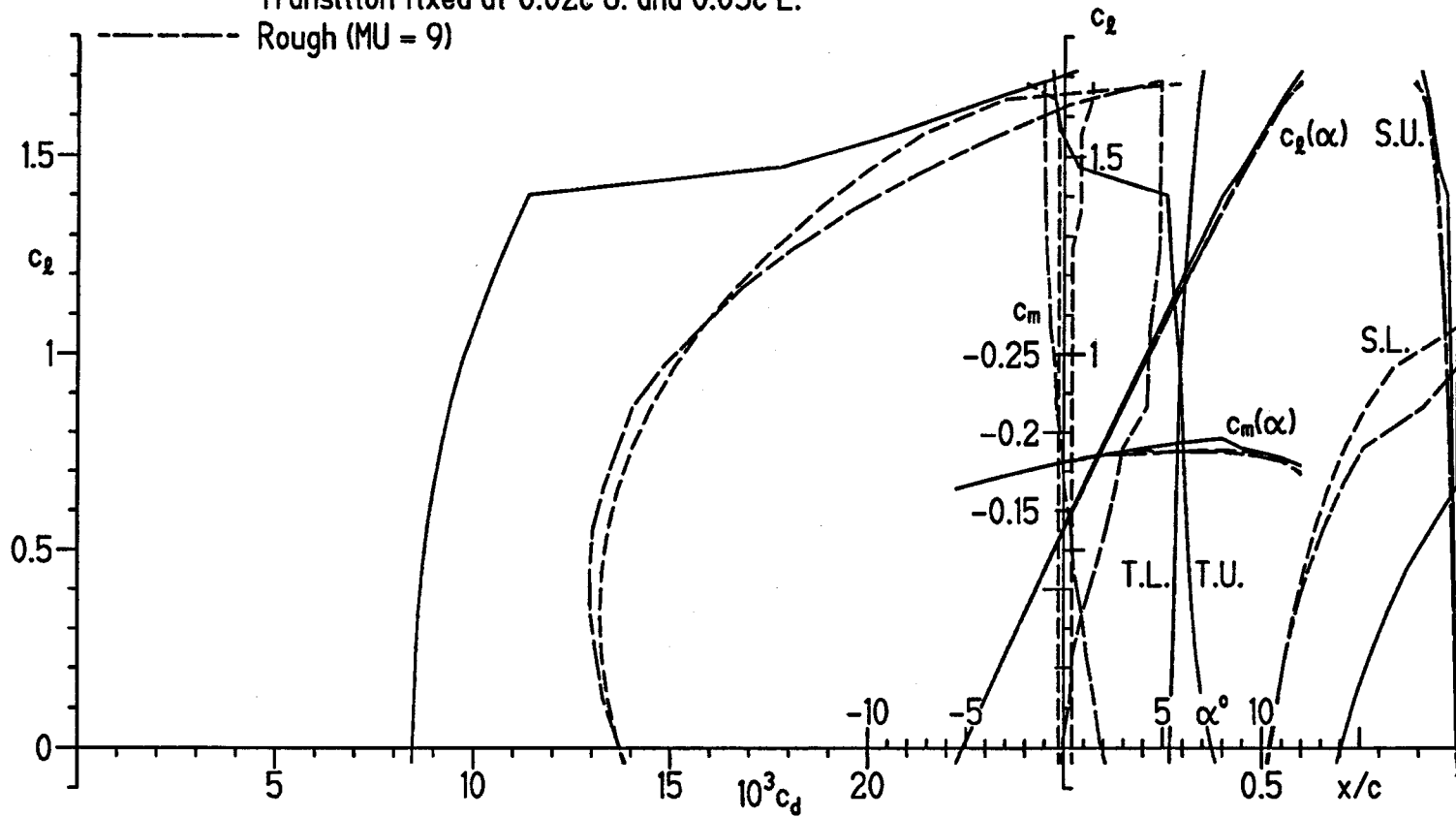
U. = upper surface

L. = lower surface

— Transition free

- - - Transition fixed at $0.02c$ U. and $0.05c$ L.

- · - · - Rough (MU = 9)



(d) $R = 3.0 \times 10^6$.

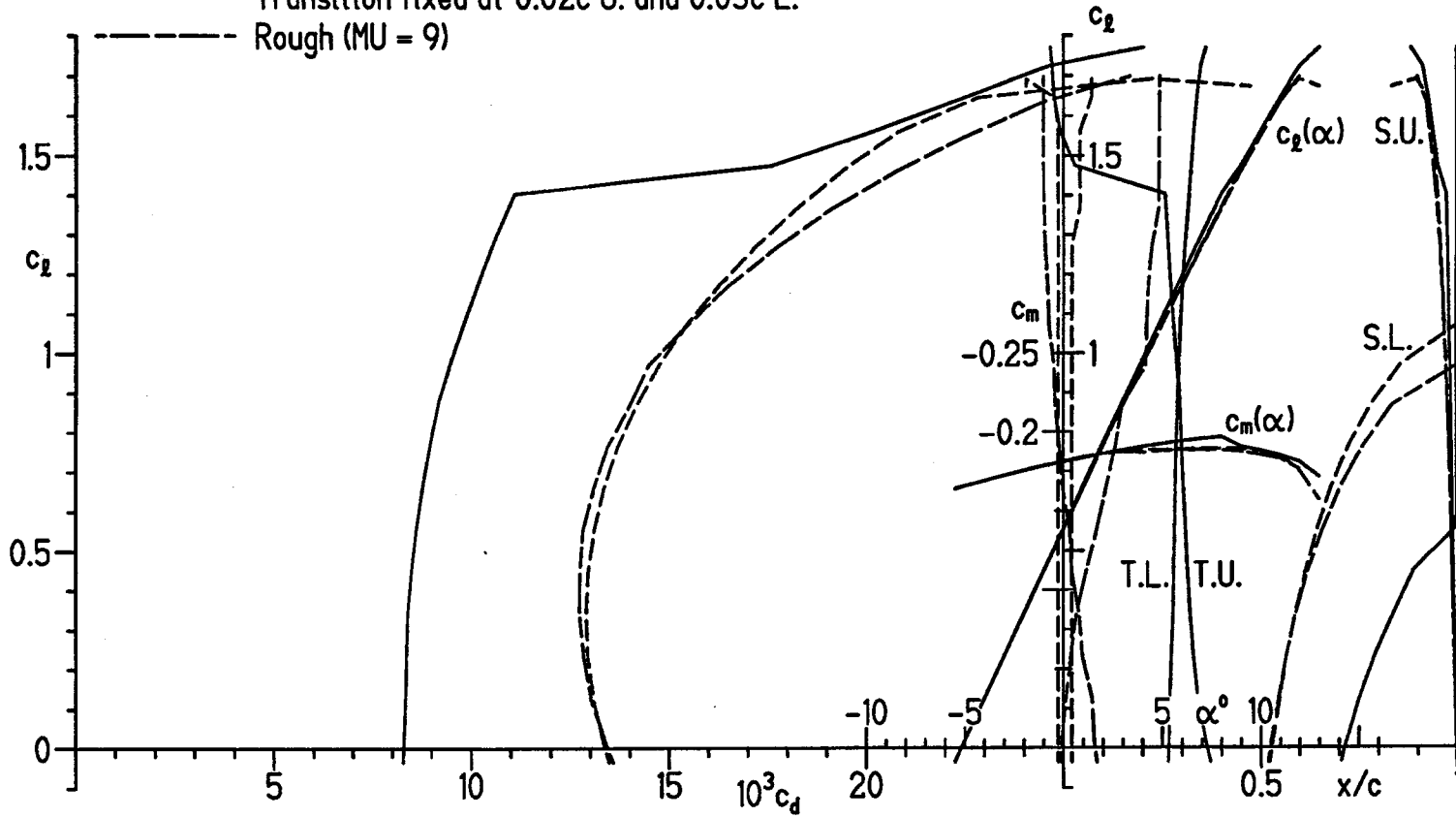
Figure 7.- Continued.

S818 $R = 3.5 \times 10^6$

Separation bubble warning
 Δ upper surface
 ∇ lower surface

T. = boundary layer transition
 S. = boundary layer separation
 U. = upper surface
 L. = lower surface

— Transition free
 - - - Transition fixed at $0.02c$ U. and $0.05c$ L.
 - - - Rough (MU = 9)



(e) $R = 3.5 \times 10^6$.

Figure 7.- Concluded.

REPORT DOCUMENTATION PAGE

Form Approved
OMB No. 0704-0188

The public reporting burden for this collection of information is estimated to average 1 hour per response, including the time for reviewing instructions, searching existing data sources, gathering and maintaining the data needed, and completing and reviewing the collection of information. Send comments regarding this burden estimate or any other aspect of this collection of information, including suggestions for reducing the burden, to Department of Defense, Executive Services and Communications Directorate (0704-0188). Respondents should be aware that notwithstanding any other provision of law, no person shall be subject to any penalty for failing to comply with a collection of information if it does not display a currently valid OMB control number.

PLEASE DO NOT RETURN YOUR FORM TO THE ABOVE ORGANIZATION.

1. REPORT DATE (DD-MM-YYYY) December 2004			2. REPORT TYPE Subcontract Report			3. DATES COVERED (From - To) October 1991 – July 1992		
4. TITLE AND SUBTITLE The S816, S817, and S818 Airfoils					5a. CONTRACT NUMBER DE-AC36-99-GO10337			
					5b. GRANT NUMBER			
					5c. PROGRAM ELEMENT NUMBER			
6. AUTHOR(S) D.M. Somers					5d. PROJECT NUMBER NREL/SR-500-36333			
					5e. TASK NUMBER WER43110			
					5f. WORK UNIT NUMBER			
7. PERFORMING ORGANIZATION NAME(S) AND ADDRESS(ES) Airfoils, Inc., 601 Cricklewood Drive State College, PA 16083						8. PERFORMING ORGANIZATION REPORT NUMBER AF-1-11154-1		
9. SPONSORING/MONITORING AGENCY NAME(S) AND ADDRESS(ES) National Renewable Energy Laboratory 1617 Cole Blvd. Golden, CO 80401-3393						10. SPONSOR/MONITOR'S ACRONYM(S) NREL		
						11. SPONSORING/MONITORING AGENCY REPORT NUMBER NREL/SR-500-36333		
12. DISTRIBUTION AVAILABILITY STATEMENT National Technical Information Service U.S. Department of Commerce 5285 Port Royal Road Springfield, VA 22161								
13. SUPPLEMENTARY NOTES NREL Technical Monitor: J. Tangler								
14. ABSTRACT (Maximum 200 Words) A family of thick laminar-flow airfoils for 30 to 40-meter horizontal-axis wind turbines, the S816, S817, and S818, has been designed and analyzed theoretically. The primary objectives of restrained maximum lift, insensitive to roughness, and low profile drag have been achieved. The constraints on the pitching moments and airfoil thicknesses have been satisfied.								
15. SUBJECT TERMS wind turbine; wind turbine airfoil design; laminar-flow airfoils;								
16. SECURITY CLASSIFICATION OF:			17. LIMITATION OF ABSTRACT UL	18. NUMBER OF PAGES	19a. NAME OF RESPONSIBLE PERSON			
a. REPORT Unclassified	b. ABSTRACT Unclassified	c. THIS PAGE Unclassified			19b. TELEPHONE NUMBER (Include area code)			

Standard Form 298 (Rev. 8/98)
Prescribed by ANSI Std. Z39.18